JOURNAL OF VIROLOGY, Aug. 1996, p. 5312–5328 Vol. 70, No. 8
0022-538X/96/$04.00+0

Two Distinct Upstream Regulatory Domains Containing Multicopy Cellular Transcription Factor Binding Sites Provide Basal Repression and Inducible Enhancer Characteristics to the Immediate-Early IES (US3) Promoter from Human Cytomegalovirus

YU-JIUN CHAN, WEN-PING TSENG, AND GARY S. HAYWARD*

The Molecular Virology Laboratories, Departments of Pharmacology and Molecular Sciences and Oncology, Johns Hopkins University School of Medicine, Baltimore, Maryland 21205

Received 11 March 1996/Accepted 17 May 1996

The US3 gene of human cytomegalovirus (HCMV) is expressed at immediate-early (IE) times in permissive HF cells, but not in nonpermissive rodent cells, and encodes several proteins that have been reported to have regulatory characteristics, although they are dispensable for growth in cell culture. Both spliced and unspliced forms of US3 IE transcripts are associated with the second of only two known large and complex upstream enhancer domains within the 229-kb HCMV genome, which we refer to as the IES *cis*-acting control region. Only the 260-bp proximal segment (from −313 to −55) of the 600-bp IES control domain, which contains multicopy NF-κB binding sites, proved to be necessary to transfer both high basal expression plus phorbol ester- and okadaic acid-inducible characteristics to heterologous promoters in transient assays in U-937 and K-562 cells. However, the IES control region contains a distinctive 280-bp distal domain, characterized by the presence of seven interspersed repeats of a 10-bp TGTCGCGACA palindromic consensus motif that encompasses a *Nru*I site. This far upstream *Nru* repeat region (from −596 to −314) imparted up to 20-fold down-regulation effects onto strong basal heterologous promoters as well as onto the IES enhancer plus minimal promoter region in both U-937 and K-562 cells. Functional *Nru* repressor elements (NREs) could not be generated by multimerizing either the palindromic (P) *Nru* motifs alone or adjacent degenerate interrupted (I) *Nru* motifs alone. However, multimerized forms of the combined P plus I elements reconstituted the full 20-fold *cis*-acting down-regulation phenotype of the intact NRE domain. The P and I forms of the *Nru* elements each bound independently and specifically to related cellular DNA-binding factors to form differently migrating A or B complexes, respectively, whereas the combined P plus I elements bound cooperatively to both the A and B complexes with high affinity. Interestingly, nuclear extracts from U-937, K-562, HeLa, and Vero cells all formed both the A and B NRE binding factor complexes, whereas those from HF cells produced only A complexes, and Raji, HL60, and BALB/c 3T3 cells lacked both types of binding factor complexes. The core pentameric CGACA and CGATA half sites present in both the P and I *Nru* motifs are related to recently described *Drosophila* chromosomal insulator binding sites. Therefore, in addition to its *cis*-repression or silencer characteristics, the NRE domain appears likely to act to shield adjacent segments of the viral genome from the chromatin-reorganizing effects of the IES-inducible enhancer. We speculate that differential expression and regulation of the IES enhancer-controlled US3 protein, either in concert with or separately from the major IE (MIE) enhancer-controlled IE1 and IE2 transactivator proteins, may play a critical role in determining HCMV permissiveness in some cell types and perhaps also in the establishment of or reactivation from latency.

Much of the current research on latency and chronic or persistent infection of human cytomegalovirus (HCMV) in peripheral blood mononuclear cells is focused on monocyte/macrophage and myeloid precursor cell types, in which the major immediate-early (MIE) regulatory genes appear to be repressed but respond to positive up-regulation by differentiation events and signal transduction reagents, including phorbol esters (TPA) and tumor necrosis factor alpha (TNFα) (24, 31, 52, 53, 60). We have shown elsewhere that TPA treatment after infection of nonpermissive monocytoid U-937 cells provides a model system whereby the MIE gene encoding the IE1 and IE2 proteins of both HCMV and simian CMV (SCMV) can be induced, leading to low levels of the full lytic cycle and progeny virion production (9). Up-regulation of the HCMV MIE enhancer and promoter region by TPA occurs through at least four distinct types of upstream enhancer elements, including NF-κB sites (46), AP-1 sites, palindromic CRE motifs (6, 18, 48), and overlapping SRF/ETS motifs (4, 7). However, many infected human cells observed in vivo (44, 57, 63, 64) as well as infected nonpermissive rodent cell culture systems (19, 28–30) display abundant synthesis of the IE1 acidic phosphoprotein and IE2 transactivator-repressor proteins, but apparently without concomitant expression of other viral gene products. Therefore, we are interested in the concept that other accessory regulatory proteins may also be required to be expressed before full lytic cycle progression can be triggered in certain cell types or during reactivation from persistent or latent infections.

In addition to the extensively characterized MIE gene region (2, 56), HCMV encodes at least three other minor IE class transcription units. Among these, the US3 gene region is also known to contain a large, complex, upstream *cis*-acting tran-

* Corresponding author. Mailing address: Department of Pharmacology and Molecular Sciences, Johns Hopkins University School of Medicine, 725 N. Wolfe St., WBSB 317, Baltimore, MD 21205. Phone: (410) 955-8684. Fax: (410) 955-8685. Electronic mail address: Gary.Hayward@qmail.bs.jhu.edu.

scriptional enhancer domain, which we refer to as the IES control region (61, 62). However, the promoters for the two other described minor IE genes of HCMV, encoding the UL36/38 (26) and the TRS1/IRS1 (49) proteins, are not known to contain equivalent specific regulatory or enhancer domains. Functional analyses by transient cotransfection chloramphenicol acetyltransferase (CAT) assays in HeLa cells have suggested that one or more of the US3 gene products can activate the cellular heat shock (hsp70) promoter but not the viral UL112 promoter, either alone or in concert with the UL36/38 gene products (11, 54). However, the molecular mechanism that underlies this transactivation property is not understood. The US3 coding region adjacent to the IES enhancer region at genome position 0.825 to 0.828 (Fig. 1A) gives rise to a 0.9-kb unspliced mRNA and several multiply spliced leftward transcripts with 3′ coterminal poly(A) tails during both IE and later stages of infection as defined by cycloheximide or anisomycin block experiments (54, 61). In our hands, synthesis of the 0.9-kb IE form of US3 mRNA peaks between 3 to 6 h after infection of permissive HF cells but does not occur after infection of nonpermissive BALB/c 3T3 cells (5, 61). Although the specific proteins encoded by the different US3 mRNAs have not yet been identified in infected cells, the predicted coding sequences suggest that the intact US3 gene product may include a membrane-associated protein domain.

The US3 gene products are not required for HCMV lytic cycle infection under normal permissive conditions in HF cell cultures (21, 23), although the temperature-sensitive HCMV mutant *ts*9, which contains a deletion from US1 through US13, failed to produce viral progeny at nonpermissive temperatures and a virus deleted in this region failed to down-regulate major histocompatibility complex class I expression (20, 23, 65). Perhaps the US3 gene products help to block or to counteract stress effects induced by infection at relatively high temperatures. However, since the US3 transcripts are controlled by the complex IES enhancer region, which we show here can be influenced by cellular transcription factors and expressed independently of the MIE proteins, it seems likely that the US3 gene products may also be involved in either cell-type-specific regulation of permissiveness or in maintenance of or reactivation from a latent state in vivo.

Weston (61) first characterized the IE mRNA encoded by the US3 region of HCMV(AD169) and identified and sequenced an associated complex upstream regulatory region in its promoter (Fig. 1A). This putative IES regulatory region displays an interesting bipartite structure consisting of two distinct blocks of repeated motifs (62). Seven copies of a novel 10-bp palindromic consensus sequence TGTCGCGACA (encompassing a core *Nru*I site) lie between positions −562 and −342, and five inverted copies of a classical NF-κB site with the consensus sequence of GGGACTTTCC occur between positions −256 and −89 (Fig. 1B). The NF-κB region in the HCMV IES promoter has been previously demonstrated to give high basal activity in HeLa cells (61). However, no function was assigned to the *Nru* motif region, and there has been no information available about how this promoter is regulated.

Our work described here demonstrates that the intact upstream IES promoter control region is subject to complex regulation involving both TPA- and okadaic acid (OA)-induced signal transduction pathways and cellular basal enhancer and repressor factors. The NF-κB domain mediates the high basal activity and TPA responsiveness, and multimerized copies of the *Nru* plus adjacent *Nru*-like regulatory elements (NREs) function as basal repressors or silencers in certain cell types. We have also identified two specific cellular factors that bind to these motifs but differ in their cell type distribution. Furthermore, we show elsewhere that the IES promoter/enhancer is subject to both positive and negative regulation by the HCMV IE2 transactivator-repressor protein in a manner that is dependent on the cell type involved (5).

MATERIALS AND METHODS

Cells and reagents. Human K-562 (erythroleukemia), U-937 (monocyte-like histiocytic lymphoma), Raji (B-cell lymphoblast), and HL-60 (prepromyelocyte) cell lines were grown in suspension in RPMI 1640 medium plus 10% fetal calf serum in a 37°C incubator supplied with 5% CO_2. Adherent human HF, mouse BALB/c 3T3, and African green monkey Vero cells were grown in Dulbecco modified Eagle medium plus 10% fetal calf serum. K-562 and U-937 cells were obtained from the American Type Culture Collection (Rockville, Md.). TPA (12-*O*-tetradecanoylphorbol-13 acetate) was purchased from Sigma and dissolved in dimethyl sulfoxide to a concentration of 20 μg/ml as a stock solution and was used at a working concentration of 50 ng/ml for each TPA stimulation experiment. OA was purchased from Boehringer Mannheim Co. and dissolved in ethanol as 100× stock solutions and added at the described concentrations. Large-scale HeLa and U-937 cell preparations for nuclear extracts were purchased from the Cell Culture Center (Cellex Biosciences Inc., Minneapolis, Minn.).

Plasmids and reporter gene constructs. Plasmid pCJC81 containing the minimal SCMV(Colburn) MIE promoter region (MIEm) from −69 to +30 in front of a CAT reporter cassette with a *Bgl*II linker site has been described previously (7). The full-length HCMV IES promoter/enhancer gene construction NE/IES-CAT (−596 to +80) in plasmid pYJC94A was generated by PCR techniques from pRL105 (Towne *Hin*dIII-E fragment; 17.2 kb) using primers LGH449 and LGH450 to generate a 686-bp (NE/IES) DNA fragment (between genome coordinates 194691 to 195376), which was digested with *Bam*HI plus *Bgl*II and subsequently cloned into a *Bam*HI site in the reporter gene vector plasmid pCATB′. The same PCR fragment was digested with *Eco*RV or *Eco*RV plus *Sna*BI to generate the intact upstream *Nru* (N) domain (−596/−314), the intact NF-κB (E) enhancer domain (−313/−55), or the NF-κB plus minimal promoter and TATA (E/IES) fragment (−313/+80). A 12-mer *Bam*HI linker was added to the 5′ end of the E/IES fragment, or an 8-mer *Bam*HI linker was added to the 3′ end of the *Nru* domain and to both the 5′ and 3′ ends of the NF-κB domain. The E/IES fragment was then cloned into a *Bam*HI site in pCATB′ to generate the E/IES-CAT gene in plasmid pYJC93A. The *Nru* and NF-κB domains were cloned into the *Bam*HI site of a pUC18-based vector (pGH56) to generate N and E cassettes in plasmids pYJC82 and pYJC81, respectively, and were then subcloned into the *Bgl*II site of the SCMV MIEm(−69/+33)-CAT gene in pCJC81 to give pYJC92 (containing the N domain) and pYJC91 (containing the E domain). Plasmid pYJC90 containing the minimal IES(−54/+80)-CAT gene was generated by deletion of plasmid pYJC94A between *Bam*HI and *Sna*BI, with the addition of a 12-mer *Bam*HI linker followed by *Bam*HI digestion and religation. The intact NE/IES and the truncated E/IES fragments were also cloned into a *Bgl*II site in the pGL2-BAS vector (13) containing a luciferase (LUC) reporter gene to generate the NE/IES-LUC gene in pYJC94L and the E/IES-LUC gene in pYJC93L.

Plasmid pCJC114b contains four copies of the synthetic SNE (SRF/ETS) motif oligonucleotides LGH218/219 placed in the backward orientation at the 5′ *Bgl*II site at −69 in the SCMV MIEm(−69/+30)-CAT gene of pCJC81 (7). Six tandemly repeated copies of a series of different synthetic oligonucleotide derivatives of the *Nru* repressor elements (LGH895/534, -647/648, -1243/1244, etc.; Table 1 and the legend to Fig. 6) were cloned into either the 5′ *Bgl*II site of pCJC114b or the 5′ *Bam*HI site of pYJC93A to give plasmids pYJC606A, pWPT15A, pWPT16A, and pWPT17A in the E/IES(−313/+80)-CAT background or pYJC156A, pYJC586A, pYJC636A, pYJC646A, pYJC656A, pYJC726A, pYJC846A, pYJC856A, pYJC866A, pYJC866B, and pYJC886A in the $(SNE)_4$/MIEm(−69/+30)-CAT background. Reporter genes containing the intact HCMV (−760/+10) and SCMV (−633/+30) MIE enhancer/promoter regions in front of CAT were described previously (6, 42, 50). The human immunodeficiency virus (HIV) long terminal repeat (LTR)-CAT target genes referred to as wild-type LTR(−453/+80)-CAT in plasmid pUR-III and LTR(−453/+80 ΔNFκB)-CAT in mpUR-III containing 3-bp mutations in both copies of the NF-κB motifs were described by Nabel and Baltimore (38).

Transient DNA transfection. CAT assays were carried out as described previously (40). Cells were pelleted in a microcentrifuge at 20°C for 1 min at 15,600 × *g*, washed with 1 ml of harvest buffer (40 mM Tris-HCl [pH 8.0], 150 mM NaCl, and 1 mM EDTA), repelleted, frozen and thawed three times in 100 μl of 250 mM Tris-HCl, pH 7.9 (plus 1 mM dithiothreitol [DTT] when cotransfected with LUC reporter genes), and spun down in a microcentrifuge at 4°C for 10 min at 15,600 × *g*. Assay reactions were carried out with 75 μl of either undiluted or 5-, 10-, or 20-fold diluted samples of supernatant in 150 μl of 590 mM Tris-HCl, pH 7.9–533 μM acetyl-coenzyme A–0.1 μCi of [^{14}C]chloramphenicol at 37°C for 1 h. Chloramphenicol was extracted from the aqueous phase with 1 ml of ethyl acetate by vigorously vortexing and centrifugating at 12,000 rpm for 3 min at 20°C, followed by drying in a vacuum centrifuge and resuspending in 20 μl of ethyl acetate. Acetylated and nonacetylated forms of chloramphenicol were separated by thin-layer silica gel chromatography (TLC) on glass plates (20 cm

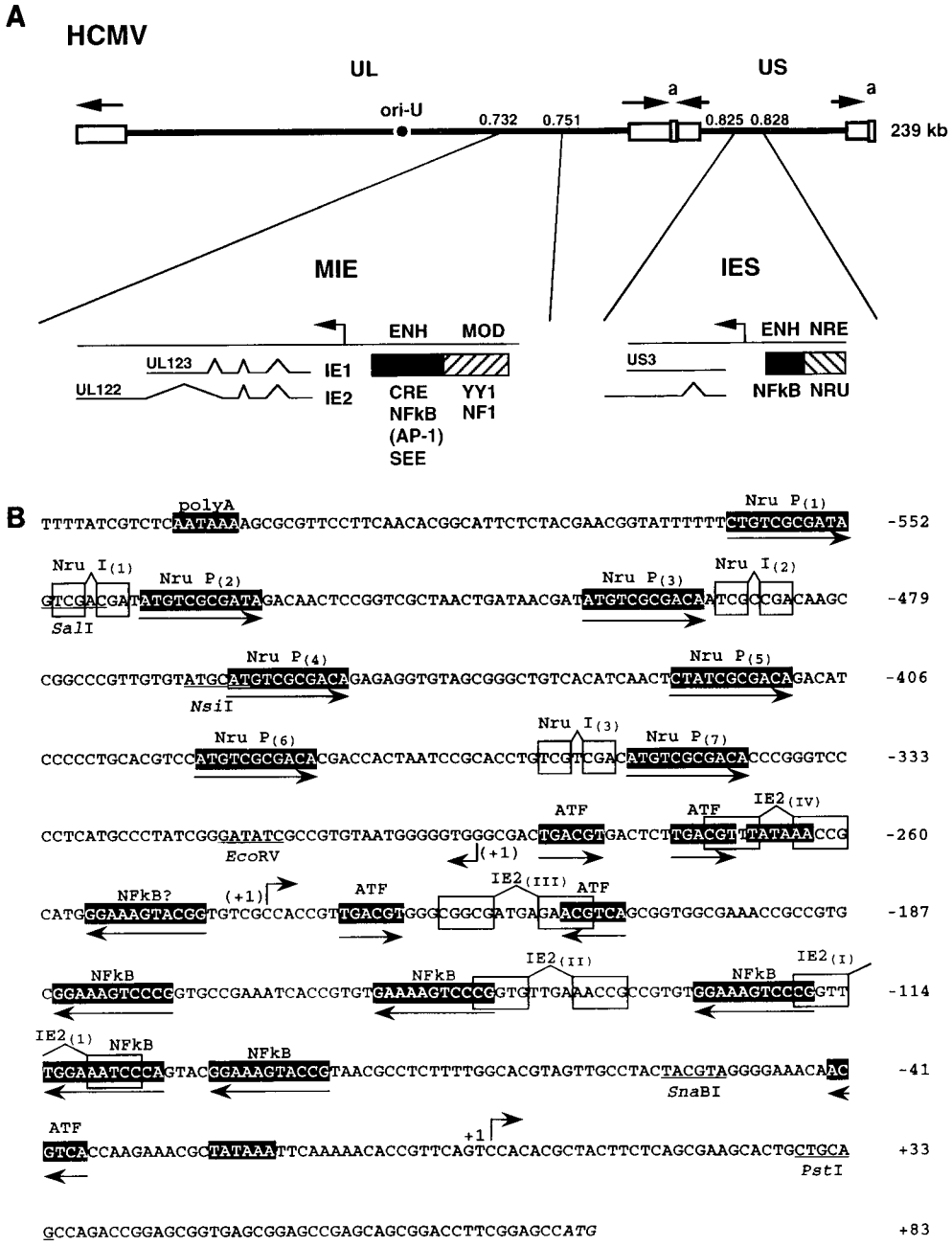

FIG. 1. (A) Relative genomic locations of the two known complex HCMV IE *cis*-acting enhancer domains MIE and IES. The MIE upstream enhancer controls expression of the abundant IE1 acidic protein (UL123) and the IE2 transactivator-repressor protein (UL122) that are both transcribed leftward with common N-terminal exons from the MIE transcription unit in UL. The IES enhancer is believed to regulate expression of the 900-bp US3 mRNA and the as yet unidentified US3 minor IE accessory transactivator protein(s) that is transcribed leftward from within US. The MIE enhancer contains TPA-inducible NF-κB, AP-1, and SEE (SRE/ETS) motifs, plus TPA- and cAMP-inducible CRE motifs, and the distal negative modulatory region (MOD), whereas as described here, the IES region contains a TPA-inducible proximal NF-κB domain (ENH) and the more distal negative *Nru* repressor domain (NRE). Ori-U refers to the location of the HCMV lytic origin in UL. (B) DNA sequence organization and location of predicted regulatory motifs within the 700-bp HCMV(Towne) IES promoter/enhancer region. The TATAAA box and ATG initiator for the US3 open reading frame (ORF) are positioned at −25 to −20 and +81 to +83 relative to the start site of transcription (+1 arrow). Two additional potential TATAAA motifs (one in each direction) lie at position −270 to −264 between the *Nru* and NF-κB domains. A potential poly(A) signal associated with the upstream US4 ORF transcript at −610 defines the outside boundary of the intact IES domain. The seven palindromic *Nru* motifs (numbered $P_{(1)}$ to $P_{(7)}$) and the three interrupted *Nru* motifs (numbered $I_{(1)}$ to $I_{(3)}$) lying between positions −562 and −342 are indicated. The *Eco*RV site at position −316 to −311 operationally defines the boundary between the *Nru* (NRE) and NF-κB (ENH) domains. The basal enhancer domain lies between −313 and −55 (*Eco*RV to *Sna*BI) and contains the five (or six?) boxed classical NF-κB consensus motifs (all in inverted orientation). Five potential ATF or half CRE motifs (TGACGT) that are commonly found near to TATAAA motifs in most HCMV promoters are also indicated. In addition, the positions of the four identified upstream binding sites for the HCMV IE2 transactivator-repressor protein (double boxes, I to IV) within the enhancer domain are indicated (59a).

by 20 cm by 0.5 mm), using chloroform-methanol at 19:1 as a solvent for 1 h.The radioactive spots were visualized by autoradiography and scraped off the TLC plates for measurement in a scintillation counter. Where appropriate, nonlinear fold effects from undiluted samples were recalculated by extrapolation from measurements with diluted samples (e.g., Fig. 2C).

LUC assays. Plasmids containing the LUC reporter gene were transfected into U-937 cells by the transient DEAE-dextran method as described above. Cells were harvested at 40 to 44 h. Each sample was resuspended in 100 μl of 0.25 M Tris-HCl (pH 7.9) plus 1 mM DTT and then disrupted by freeze-thawing. The LUC assays were carried out at 20°C by mixing 10 μl (4 μg) of cellular protein extract in 300 μl of reaction buffer A containing 25 mM glycyl-glycine (pH 7.8), 15 mM $MgSO_4$, 5 mM ATP, and 4 mM EGTA with 100 μl of reaction buffer B containing 1 mM of luciferin (Sigma) in reaction buffer A in the chamber of a LUMAT LB 9501 luminometer. The program was set to count the relative light units for 6 s. For each experiment, serial dilutions of standard LUC purchased from Sigma were carried out to confirm the linearity of the assay.

Labelling of synthetic oligonucleotides. Single-stranded 30-mer oligonucleotides were synthesized by Scott Morrow (Johns Hopkins University, School of Hygiene and Public Health) and purified by high-pressure liquid chromatography procedures. The two complementary strands (10 μg) of each oligonucleotide pair generated 4-bp GATC 5′ overhangs after being heated to 65°C for 5 min in 100 μl of STE (100 mM NaCl, 10 mM Tris-HCl [pH 8.0], and 1 mM EDTA) and annealed by slow cooling. The labelling reaction of 3′-recessed ends was carried out in 20 μl of solution containing 1 pmol/μl of synthetic oligonucleotide (3 μl), 10× reaction buffer (2 μl), 10 mM dGTP, dCTP, and dTTP mixture (1 μl), 3.3 pmol/μl of [α-^{32}P]dATP (1 μl; 10 μCi), 1 U/μl of the Klenow fragment of polynucleotide polymerase (1 μl), and 12 μl of H_2O at 20°C for 30 min. The labelled double-stranded oligonucleotides were separated from free nucleotides by centrifugation at 1,600 × *g* for 5 min on Sephadex G-25 columns.

EMSA. Nuclear extracts were prepared by a modified Dignam method (14). Suspension cells were collected at a density of 10^6 cells/ml, and adherent cells were harvested with rubber scrapers. The cells were washed with phosphate-buffered saline. Two packed cell volumes of buffer A containing 10 mM HEPES (*N*-2-hydroxyethylpiperazine-*N*′-2-ethanesulfonic acid) (pH 7.9), 1.5 mM $MgCl_2$, 10 mM KCl, 0.5 mM DTT, and protease inhibitor mixture (0.1 mM tolylsulfonyl phenylalanyl chloromethyl ketone, 1 mM tolylsulfonyl lysine chloromethyl ketone, 0.5 mM phenylmethylsulfonyl fluoride, 1 μg of aprotinin per ml, 1 μg of leupeptin per ml, and 1 μg of pepstatin A per ml) was added to swell the cells on ice for 10 min. A Dounce homogenizer size B (7 ml) was used to rupture the cell membranes. The nuclei were collected at 1,600 × *g* at 4°C and resuspended in high salt buffer C containing 20 mM HEPES (pH 7.9), 25% (vol/vol) glycerol, 0.42 M NaCl, 1.5 mM $MgCl_2$, 0.2 mM EDTA, 0.5 mM DTT, and the protease inhibitor mixture to extract nuclear proteins by rocking at 4°C for 1 h and removing the nuclear debris. The supernatant which contains nuclear proteins was aliquotted and stored at −70°C for later use.

DNA-protein binding reactions were set up as described previously (34, 45) in a final volume of 20 μl containing 1× ZTA buffer (10 mM HEPES [pH 7.5], 50 mM KCl, 1 mM EDTA, 0.1% TritonX- 100, 5% glycerol, 0.1 mM DTT, and 0.1 mM phenylmethylsulfonyl fluoride), 5 to 10 μg of nuclear extract, 1 μg of poly(dI-dC)-poly(dI-dC), and 5 fmol of the ^{32}P-end-labelled oligonucleotide DNA probe and incubated for 15 min at 20°C. Electrophoretic mobility shift assays (EMSA) were performed on the DNA-protein complexes in a 4% polyacrylamide gel (acrylamide-bisacrylamide ratio of 29:1) using 0.5× TBE as running buffer. Electrophoresis was carried out at 150 to 200 V for 60 to 120 min at 20°C, and the gels (18 by 20 cm) were dried for autoradiography.

RESULTS

Identification of a TPA- and OA-responsive enhancer region upstream of the HCMV IES promoter. To study the transcriptional regulation of the US3 gene, we generated a series of plasmids containing CAT or LUC reporter genes encompassing different portions of the 5′ region upstream from the HCMV (Towne) US3 open reading frame by PCR. We refer to this enhancer/promoter region as the intact IES control region (IE region in the short unique segment) (Fig. 1). To begin to determine whether the IES enhancer responded to the same or different external stimuli than does the MIE enhancer in cells of the monocyte lineage, the IES minimal promoter from −54 to +80 (IES-CAT gene) or the whole IES enhancer/promoter from −596 to +80 (NE/IES-CAT gene) was transfected into suspension cultures of human U-937 cells by the DEAE-dextran procedure. The cultures were subsequently treated with 50 ng of TPA per ml or either 2 or 50 nM OA. The latter specifically inhibits protein phosphatase 2A (PP2A activity at a very low dose (50% inhibitory concentration [IC_{50}] of <1 nM) and at a higher dose inhibits protein phosphatase 1 (PP1) activity (IC_{50} = 10 to 15 nM) (11). Without any external stimulation, the intact regulatory domain in NE/IES-CAT gave only 2.7-fold higher basal activity in U-937 cells than that of the minimal IES promoter in IES-CAT (Fig. 2A, lanes 1 and 5). However, both TPA and 50 nM OA treatment resulted in 93- and 66-fold stimulation of NE/IES-CAT activity, respectively (lanes 6 and 8). In contrast, the minimal IES promoter, IES-CAT, responded to TPA and OA only 1.3- to 1.7-fold (lanes 2 and 4). Low-dose (2 nM) OA failed to enhance the NE/IES-CAT basal activity (1.1-fold increase, lane 7). Therefore, we conclude that the IES enhancer can respond to phosphorylation state modulators including the protein kinase C pathway stimulant TPA and the phosphatase inhibitor OA.

The proximal NF-κB segment of the IES 5′-upstream region is sufficient for TPA and OA responsiveness and gives high basal enhancer activity in U-937 cells. To further dissect the regulatory region in the IES enhancer, we examined the sequence of the entire IES control region and found two distinct blocks of repetitive motifs (Fig. 1). The proximal region encompasses five or six copies of a classical consensus NF-κB binding site, GGGACTTTCC, and the distal region encompasses seven copies of a novel 10-bp palindromic consensus sequence, TGTCGCGACA. We will refer to the distal region from −596 to −314 as the *Nru* domain (N) and the proximal region from −313 to −55 as the NF-κB enhancer domain (E). Weston (61) examined the promoter strength of the NF-κB and *Nru* domains in HeLa cells by using β-globin gene reporter mRNA and concluded that the NF-κB domain gave basal enhancement but that the *Nru* domain had little effect on promoter activity. To determine whether the TPA responsiveness lies within the NF-κB domain, CAT reporter genes containing both the *Nru* and NF-κB domains (NE/IES-CAT) or the NF-κB domain alone (E/IES-CAT) were transfected into U-937 cells and assayed for CAT activity. The minimal IES promoter (IES-CAT) served as a negative control.

The initial results shown confirmed that the NF-κB domain enhanced the basal activity 16-fold in comparison with the minimal IES-CAT gene in U-937 cells (Fig. 2B, lanes 1 and 3). In addition, the NF-κB domain in E/IES-CAT responded strongly to TPA stimulation (lane 4), giving a greater than 15-fold TPA-mediated response in U-937 cells and producing higher overall activity in the presence of TPA than did the intact NE/IES-CAT gene in a parallel assay (lane 6). Furthermore, the basal activity of the E/IES-CAT plasmid was about fourfold higher than that of the NE/IES-CAT plasmid (compare lanes 3 and 5). This result implied that the distal *Nru* domain may have negative regulatory properties (see below).

Comparison with CMV MIE and HIV LTR responses. To put these results in perspective, we also compared the basal and induced levels of the three forms of IES-CAT reporter gene in U-937 cells with those of the intact HCMV and SCMV MIE enhancers and of the intact and NF-κB-mutated forms of the HIV LTR enhancer (Fig. 2C). As shown in the histogram, the basal levels of CAT activity revealed a 15-fold increase for E/IES-CAT over the minimal IES-CAT compared with 150- and 75-fold increases for the intact SCMV and HCMV MIE-CAT genes, but only 2.4-fold for HIV LTR CAT (Fig. 2C, top panel). Under conditions in which E/IES-CAT and NE/IES-CAT gave 70- and 53-fold responses to TPA and 15- and 25-fold responses to OA, respectively, the intact HCMV MIE-CAT target gave comparable 23- and 9.7-fold responses to TPA and OA and the SCMV MIE gave a 12-fold response to TPA but did not respond significantly to OA (1.6-fold). These values were all obtained with 10-fold dilutions of the extract. In contrast, the TPA-induced LTR-CAT target gave only 5% of the activity of TPA-induced HCMV MIE-CAT at a 10-fold

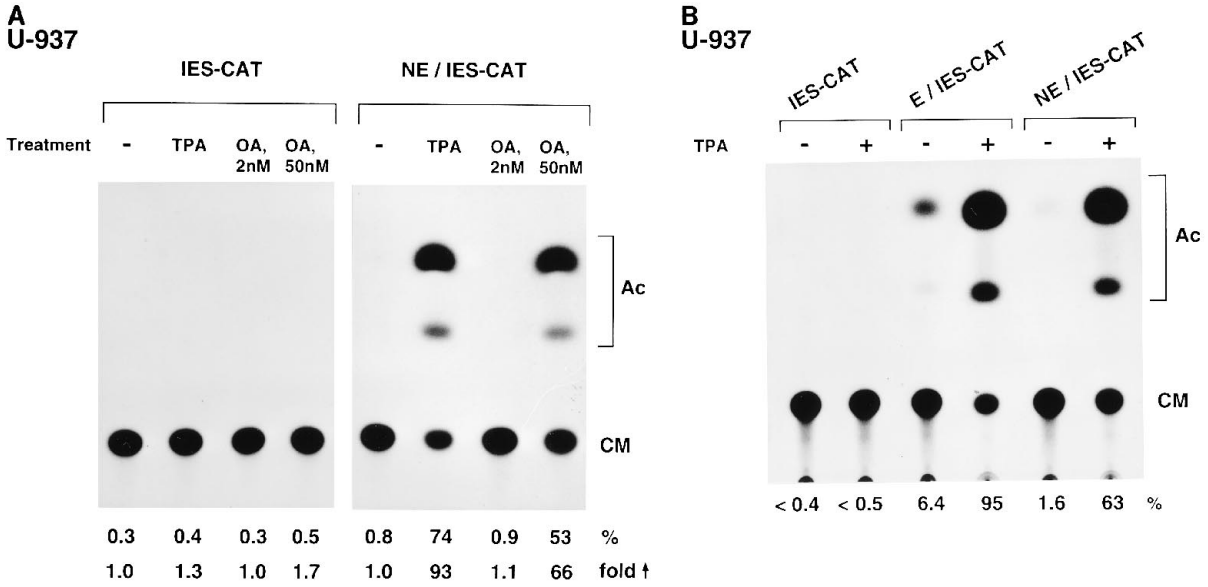

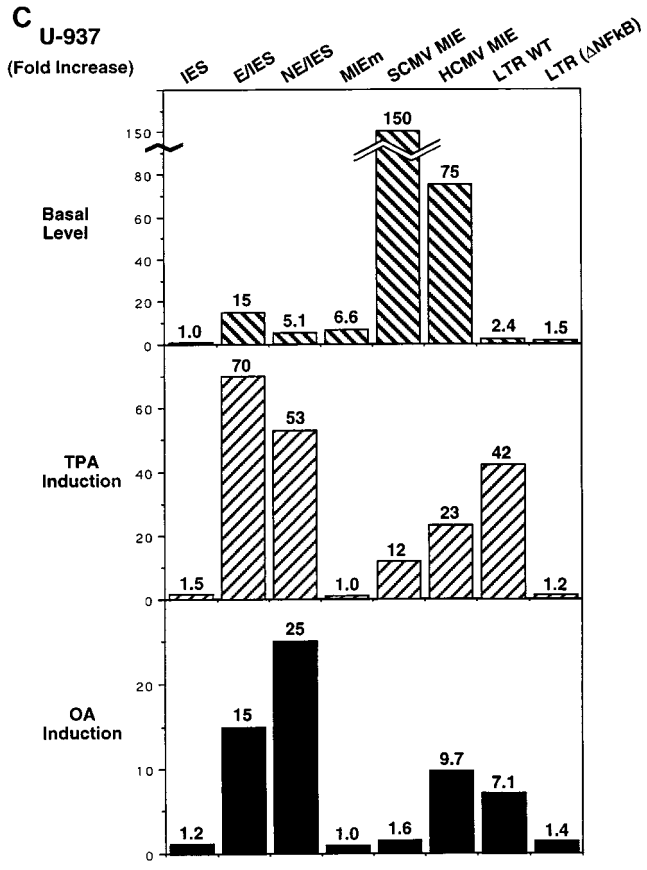

FIG. 2. (A) The HCMV IES enhancer region responds to TPA and OA stimulation in U-937 cells. Autoradiograph showing the results of transient CAT expression assays in U-937 cells after transfection of the minimal IES-CAT gene (in plasmid pYJC90) compared with those of the whole enhancer NE/IES-CAT reporter gene (pYJC94A) with and without TPA or OA treatment. TPA (50 ng/ml) or OA (2 or 50 nM) was added to the culture medium 18 h prior to harvesting. The percent conversion of [^{14}C]chloramphenicol to acetylated forms and fold induction are indicated below each lane. (B) Basal enhancement and TPA responsiveness map to the proximal NF-κB enhancer domain (E) of the IES promoter. Autoradiograph comparing the results of transient CAT expression assays in U-937 cells with those for the minimal IES-CAT gene (pYJC90), the minimal plus NF-κB domain E/IES-CAT gene (pYJC93A), and the whole *Nru* plus enhancer domain NE/IES-CAT gene (pYJC94A) in the presence or absence of TPA (50 ng/ml). (C) Histogram comparing basal levels and the results of TPA and OA treatment on the HCMV NE/IES and E/IES regions with those obtained on the HCMV and SCMV MIE and HIV LTR regions. Transfection experiments were carried out in U-937 cells with minimal IES-CAT (pYJC90), E/IES-CAT (pYJC93A), NE/IES-CAT (pYJC94A), minimal SCMV MIE(−69/+30)-CAT (pCJC81), intact SCMV MIE(−633/+30)-CAT (pDG7), HCMV MIE(−760/+10)-CAT (p760wt-CAT), intact HIV LTR-CAT (pU3RIII), or mutant HIV LTR(ΔNF-κB)-CAT (mpU3RIII). Separate panels show basal levels and response to 50 ng of TPA per ml or response to 50 nM OA. CAT results are plotted as percent conversion, using undiluted samples for most basal measurements and 10-fold diluted samples of the extracts for most TPA and OA responses. The fold increases in minimal IES-CAT basal levels or fold-induction values after TPA and OA treatment are given above the columns.

dilution (not shown). However, with undiluted extracts the minimal IES-CAT, minimal MIE-CAT, intact LTR-CAT, and LTR(ΔNF-κB)-CAT genes showed 1.5-, 1.0-, 42-, and 1.2-fold stimulation by TPA and 1.2-, 1.0-, 7.1-, and 1.4-fold stimulation by OA, respectively (Fig. 2C).

Overall, these observations showed that all three enhancer motifs tested that contain classical NF-κB motifs (five copies in E/IES-CAT and NE/IES-CAT, four copies in HCMV MIE-CAT, and two copies in LTR-CAT) gave increased basal activity and strong TPA and OA responses. Both of these responses were abolished by point mutations within the 2× NF-κB motifs in the HIV LTR(ΔNFκB)-CAT gene. Note that parallel experiments with the SCMV MIE enhancer region, which lacks classical NF-κB sites, while still being stimulated strongly by TPA, failed to produce OA responses. Sambucetti et al. (46) previously demonstrated that the NF-κB (18-bp) elements in the HCMV MIE enhancer responded to TPA in Jurkat T cells. We have also found that the addition of a two-copy tandemly repeated classical consensus wild-type NF-κB site, but not mutant NF-κB motifs, into a simian virus 40 minimal promoter CAT gene produced both OA and TPA responsiveness, as well as TNFα responsiveness and basal enhancement in U-937 cells (3, 9).

The basal enhancer and TPA-responsive characteristics of the IES NF-κB enhancer domain can be transferred to a heterologous promoter in both U-937 and K-562 cells. To confirm the observation that the proximal NF-κB domain but not the distal *Nru* domain of the IES control region gives rise to both the basal activity and TPA responsiveness, we placed

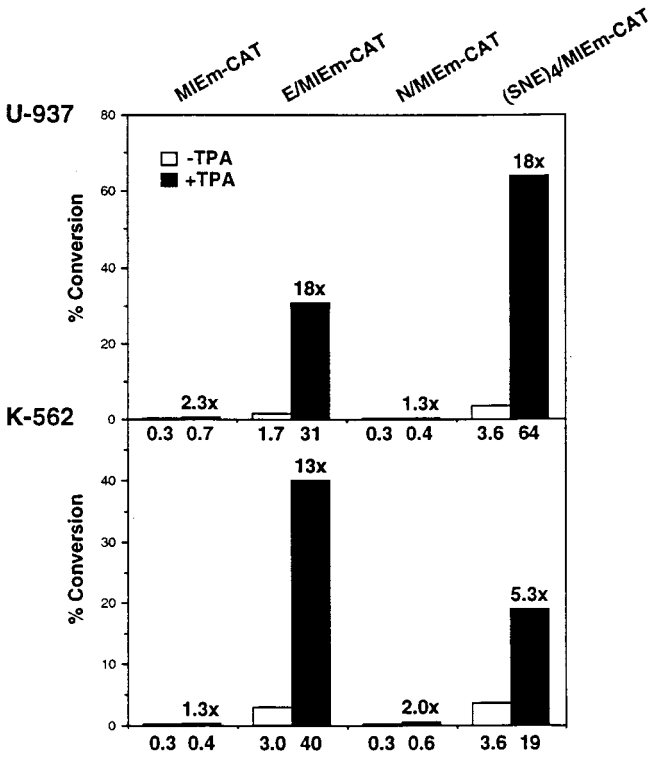

FIG. 3. The NF-κB enhancer domain (E) transfers both basal enhancement and TPA responsiveness to a heterologous promoter. The histograms compare the results of transient CAT expression assays to measure levels of TPA induction from the isolated IES, ENH(E), and NRE(N) domains placed in the minimal MIE promoter background in U-937 and K-562 cells. Samples included the parent minimal SCMV IE94 promoter CAT reporter gene (MIEm-CAT gene in pCJC81), a version with the IES NF-κB domain added (the E/MIEm-CAT gene in pYJC91), a version with the IES *Nru* domain added (the N/MIEm-CAT gene in pYJC92), and a version with four tandem copies of the 30-mer wild-type SCMV SNE (SRF/ETS) motif oligonucleotide added [the $(SNE)_4$/MIEm-CAT gene in pCJC114B]. The data are shown as percent conversion and fold-induction values measured in 10-fold diluted (U-937) or 20-fold diluted (K-562) extract samples. Open bars represent basal levels, and solid bars represent TPA-treated samples.

the isolated NF-κB and *Nru* domains separately in front of the heterologous SCMV IE94 minimal promoter, MIEm(−69/+30)-CAT, to generate E/MIEm-CAT (containing the NF-κB domain) and N/MIEm-CAT (containing the *Nru* domain). These targets were tested in a transient transfection assay in both U-937 and K-562 cells (Fig. 3), together with the known highly TPA-responsive target reporter gene $(SNE)_4$/MIEm-CAT, which contains four copies of the overlapping SRE and ETS motifs from the SCMV MIE ENH-A2 region (7). The results show that E/MIEm-CAT increased the basal level 11-fold more than the parent minimal promoter in the MIEm (−69/+30)-CAT gene and TPA treatment increased this value to 140-fold, in contrast to only 1.3-fold for the parent MIEm-CAT target. As expected, the N/MIEm-CAT plasmid neither gave high basal activity nor responded significantly to TPA stimulation. These results compare favorably with the values of 12-fold for basal and overall 67-fold with TPA for the SCMV 4× SNE motifs. Once again, these measurements all involved 10- or 20-fold dilutions of the extracts, whereas for the control LTR-CAT gene in undiluted K-562 extract samples the values were 5.7% basal and 54% after TPA treatment (9.7-fold induction) and for LTR(ΔNF/κB)-CAT the values fell dramatically to 0.5% basal and 0.6% after TPA treatment (not shown). Therefore, we conclude that both the high basal activity and TPA responsiveness are mediated exclusively by the proximal NF-κB domain, rather than by the distal *Nru* domain and that the effects were quite similar in K-562 cells and in U-937 cells.

The distal *Nru* domain functions as a negative modulator to down-regulate a high basal promoter. In the above experiments the basal activity of the E/IES-CAT gene, which contains only the NF-κB domain, was 3- to 5-fold higher than that of the NE/IES-CAT gene, which encompasses both the *Nru* domain and the NF-κB domain (Fig. 2B and C). This result implied that the *Nru* domain might negatively regulate the basal activity of the IES promoter. Therefore, to ask whether the *Nru* domain serves as an independent transferrable negative regulatory region, we moved the *Nru* domain (N) into 5′ upstream locations in two well-defined heterologous reporter genes having moderate and very high basal activity, respectively. Initially, it was placed at position −69 in the minimal SCMV MIE promoter background as described above and both basal and TPA-induced activities were measured in undiluted K-562 extracts. The results again revealed an at least fivefold basal repression effect by the *Nru* domain (N) compared with a 12-fold basal stimulation by the NF-κB enhancer domain (E) (Fig. 4A). Second, the *Nru* domain was placed at position −190 in a parent $(SNE)_4$/MIEm-CAT gene, which contains four added upstream tandem copies of a 30-bp synthetic oligonucleotide pair encompassing overlapping SRF and ETS binding sites from the SCMV MIE gene (4, 7) and provides both high basal enhancer activity and TPA responsiveness (Fig. 3).

This new target gene, N/$(SNE)_4$/MIEm-CAT, was tested together with its parent and appropriate control reporter genes containing different segments of the IES enhancer and minimal promoter regions in a transient transfection assay in U-937 cells. Again, the basal activity was reduced fourfold for the natural context NE/IES-CAT control compared with E/IES-CAT (Fig. 4B, upper panel). Furthermore, the down-regulation effect of the *Nru* domain proved to be transferrable to the enhanced heterologous system in which it reduced the basal activity of the $(SNE)_4$/MIEm-CAT gene by 6.2-fold [compare $(SNE)_4$/MIEm-CAT and N/$(SNE)_4$/MIEm-CAT in Fig. 4B, upper panel]. In both backgrounds, the overall activity after TPA treatment was also lower by 4.4-fold in the presence of the *Nru* domain (Fig. 4B, center panel), whereas the actual TPA-induction responses of these target genes were all in the range of 20- to 40-fold in diluted extracts (Fig. 4B, lower panel). In contrast, expression from the minimal IES-CAT gene increased only 1.3-fold after TPA stimulation. Therefore, the negative effect of the *cis*-acting *Nru* domain persisted after TPA stimulation, and the *Nru* domain apparently neither impeded nor augmented the TPA responsiveness of either its natural adjacent NF-κB proximal domain nor that of the synthetic SNE motifs.

To confirm that the lower basal activity seen in the CAT reporter gene containing the *Nru* domain was not caused either by experimental error related to variations of transfection efficiency or to reporter gene specific effects, a reciprocal dose-response experiment was performed by cotransfecting either a LUC reporter gene driven by the NF-κB domain (E/IES-LUC) and a CAT reporter gene driven by the NF-κB plus *Nru* domain (NE/IES-CAT) or the reciprocal paired combination of a LUC gene driven by the NF-κB plus *Nru* domain (NE/IES-LUC) and a CAT gene driven by the NF-κB domain (E/IES-CAT). In each sample, the combined total amount of the two input plasmid DNAs was adjusted to 4 μg, with gradual increases in the amounts of the CAT reporter genes from 0 to 4 μg concomitant with parallel decreases in the amounts of the

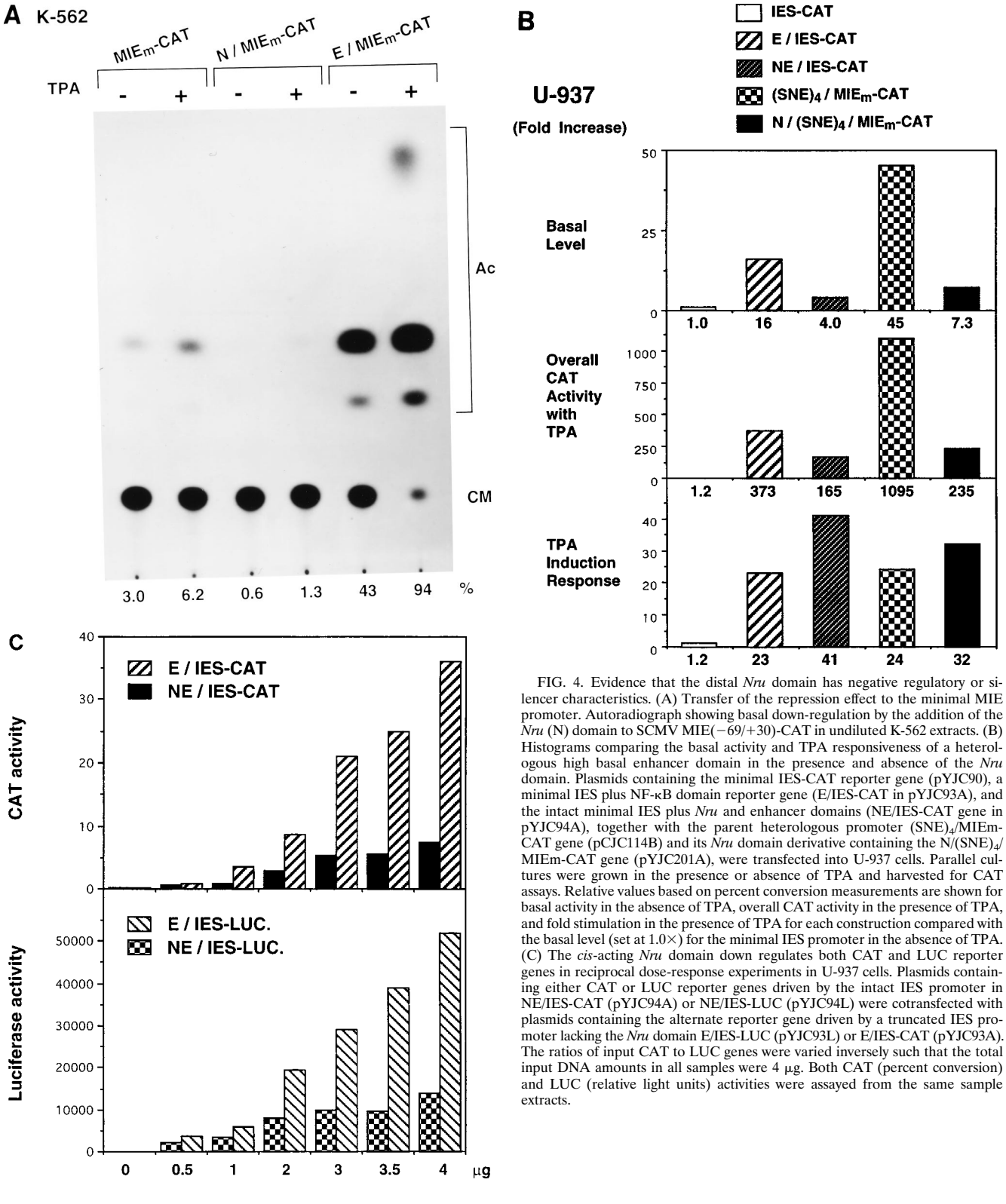

FIG. 4. Evidence that the distal *Nru* domain has negative regulatory or silencer characteristics. (A) Transfer of the repression effect to the minimal MIE promoter. Autoradiograph showing basal down-regulation by the addition of the *Nru* (N) domain to SCMV MIE(−69/+30)-CAT in undiluted K-562 extracts. (B) Histograms comparing the basal activity and TPA responsiveness of a heterologous high basal enhancer domain in the presence and absence of the *Nru* domain. Plasmids containing the minimal IES-CAT reporter gene (pYJC90), a minimal IES plus NF-κB domain reporter gene (E/IES-CAT in pYJC93A), and the intact minimal IES plus *Nru* and enhancer domains (NE/IES-CAT gene in pYJC94A), together with the parent heterologous promoter $(SNE)_4$/MIEm-CAT gene (pCJC114B) and its *Nru* domain derivative containing the N/$(SNE)_4$/MIEm-CAT gene (pYJC201A), were transfected into U-937 cells. Parallel cultures were grown in the presence or absence of TPA and harvested for CAT assays. Relative values based on percent conversion measurements are shown for basal activity in the absence of TPA, overall CAT activity in the presence of TPA, and fold stimulation in the presence of TPA for each construction compared with the basal level (set at 1.0×) for the minimal IES promoter in the absence of TPA. (C) The *cis*-acting *Nru* domain down regulates both CAT and LUC reporter genes in reciprocal dose-response experiments in U-937 cells. Plasmids containing either CAT or LUC reporter genes driven by the intact IES promoter in NE/IES-CAT (pYJC94A) or NE/IES-LUC (pYJC94L) were cotransfected with plasmids containing the alternate reporter gene driven by a truncated IES promoter lacking the *Nru* domain E/IES-LUC (pYJC93L) or E/IES-CAT (pYJC93A). The ratios of input CAT to LUC genes were varied inversely such that the total input DNA amounts in all samples were 4 μg. Both CAT (percent conversion) and LUC (relative light units) activities were assayed from the same sample extracts.

TABLE 1. Mutant *Nru* oligonucleotide motifs

Site name	Probe name	Oligonucleotide pair number and sequence (top strand only shown)	DNA-bound complex		Repression
			A	B	
		12345 678910			
WT0	P_0	895/534 GATCCACATGTCG-CGACAGGTACCAGCTGA	++	−	+
PM1	pm1	535/536 GATCCACATGTAC-GTACAGGTACCAGCTGA	−	−	−
PM2	pm2	647/648 GATCCACATTGCG-CGCAAGGTACCAGCTGA	−	−	−
PM3	pm3	805/806 GATCCTGTTGTCG-CGACATTGCACAGCTGA	++	−	ND
PM4	pm4	891/892 GATCCTGTTGTCG-CGACAGGTACCAGCTGA	(+)	ND	ND
PM5	pm5	893/894 GATCCACATGTCG-CGACATTGCACAGCTGA	(+)	ND	ND
WT1	P_1^+	1243/1244 GATCCTTCTGTCG-CGATAGTCGACAGCTGA	++	+	++
WT1-Ext	P_1I	1267/1268 GATCCTTCTGTCG-CGATAGTCGACGACTGA	+/−	++++	+++
PM6	P_{1m}^+	1249/1250 GATCCTTCTGTAC-GTATAGTCGACAGCTGA	−	−	−
WT3	P_3^+	1245/1246 GATCCATATGTCG-CGACAATCGCCAGCTGA	++	++	++
PM7	P_{3m1}^+	1251/1252 GATCCATATGTAC-GTACAATCGCCAGCTGA	−	−	ND
PM8	P_{3m2}^+	1253/1254 GATCCATATTGCG-CGCAAATCGCCAGCTGA	−	−	ND
PM9	I^+	1257/1258 GATCCATATGTCGTCGACAATCGCCAGCTGA	−	+++	−
WT7	P_7	1247/1248 GATCCACATGTCG-CGACACCCGGCAGCTGA	++	−	+
Ext-WT7	IP_7	1259/1260 GATCCCTGTCGTCGACATGTCG-CGACACCA	+/−	++++	+++
PM10	IP_{7m}	1263/1264 GATCCCTGTCGTCGACATGTAC-GTACACCA	−	+/−	+/−
PM11	I_mP_7	1265/1266 GATCCCTGTACTGTACATGTCG-CGACACCA	++	+/−	+

LUC reporter gene DNA. A histogram of the results (Fig. 4C) shows that both versions of the target gene that contained only the NF-κB domain always gave higher CAT or LUC activities than those containing the additional *Nru* domain sequences, irrespective of which reporter gene was used. Therefore, we conclude that the distal *Nru* domain contains transferable *cis*-acting NREs, which function to down-regulate the basal IES promoter activity.

Multimerized copies of individual *Nru* motif elements act as mediators of the *cis*-acting repression phenotype. Since the entire 282-bp *Nru* domain appeared to display a basal down-regulation phenotype in our above experiments, we suspected that the TGTCGCGACA repeats (61), which we refer to as palindromic *Nru* elements (P), might themselves act as negative *cis*-acting elements (NREs). Therefore, we generated several initial tandemly repeated synthetic 30-bp oligonucleotides encompassing the 10-bp consensus *Nru* motifs (referred to as WT0 and PM1 to PM5; Table 1) and inserted them at 5′ positions into two types of CAT reporter genes that give high basal activity, namely $(SNE)_4$/MIEm-CAT and E/IES-CAT. These were subsequently transfected into U-937 or K-562 cells for comparative measurement of transient expression levels. However, a representative result with the $(WT0)_6/(SNE)_4$/MIEm-CAT gene containing six copies of the wild-type consensus palindromic *Nru* motif (WT0) showed that it down-regulated the basal activity only 2.6-fold (Fig. 5A, lane 6) in contrast to the whole *Nru* domain, which on this occasion reduced the basal activity 16-fold in a parallel sample (lanes 1 and 2). Furthermore, $(PM2)_6/(SNE)_4$/MIEm-CAT containing mutated *Nru* motifs also reduced the basal activity 2.5-fold (lane 7), indicating that the core palindromic *Nru* motif alone was not sufficient to specifically suppress the basal activity.

To determine what kind of *Nru* motif from the distal IES domain is necessary for mediating down-regulation in transient transfection CAT assays, we also used multimerized oligonucleotides representing three larger 18-bp native *Nru* sequences (WT1, WT3, and WT7) chosen from among the seven *Nru* motifs in the IES control region (Fig. 1B). Two of these new target genes $(WT1)_6/(SNE)_4$/MIEm-CAT and $(WT3)_6/(SNE)_4$/MIEm-CAT, which contained wild-type *Nru* sites 1 and 3, showed two- to threefold less basal CAT activity than the $(WT7)_6/(SNE)_4$/MIEm-CAT gene containing site 7 (Fig. 5A, lanes 3, 4, and 5). Since they all encompass intact core 10-bp palindromic *Nru* motifs, we speculated that additional sequences flanking the palindromic *Nru* motifs must be required for repressor activity. However, the basal CAT activity of the $(WT1)_6/(SNE)_4$/MIEm-CAT or $(WT3)_6/(SNE)_4$/MIEm-CAT gene in U-937 cells was still twofold higher than that of the target gene containing the whole *Nru* domain in $N/(SNE)_4$/MIEm-CAT (lane 2). By scrutinizing the IES enhancer sequence, we identified three additional related interrupted *Nru* motifs (I) with the core sequence TCGNCGA that flank four out of the seven palindromic *Nru* motifs and are labeled I_1, I_2, and I_3 in Fig. 1B. The two most active oligonucleotides used (i.e., WT1 and WT3 but not WT7) both happened to include at least half of one of the interrupted *Nru* sequences adjacent to the 10-bp palindromic motif (Table 1).

Mutational analysis of P, I, and P plus I class *Nru* motifs. To further evaluate the role of adjacent interrupted *Nru* sequences, we generated a series of eight additional NRE-related oligonucleotides for insertion into CAT reporter genes. For example, the $(WT1\text{-}Ext)_6/(SNE)_4$/MIEm-CAT gene contains six copies of an extended palindromic *Nru* motif with the intact interrupted *Nru* sequence located 3′ to the palindromic *Nru* site 1 and placed in either a forward (A) or backward (B) orientation relative to the $(SNE)_4$/MIEm-CAT promoter. Sim-

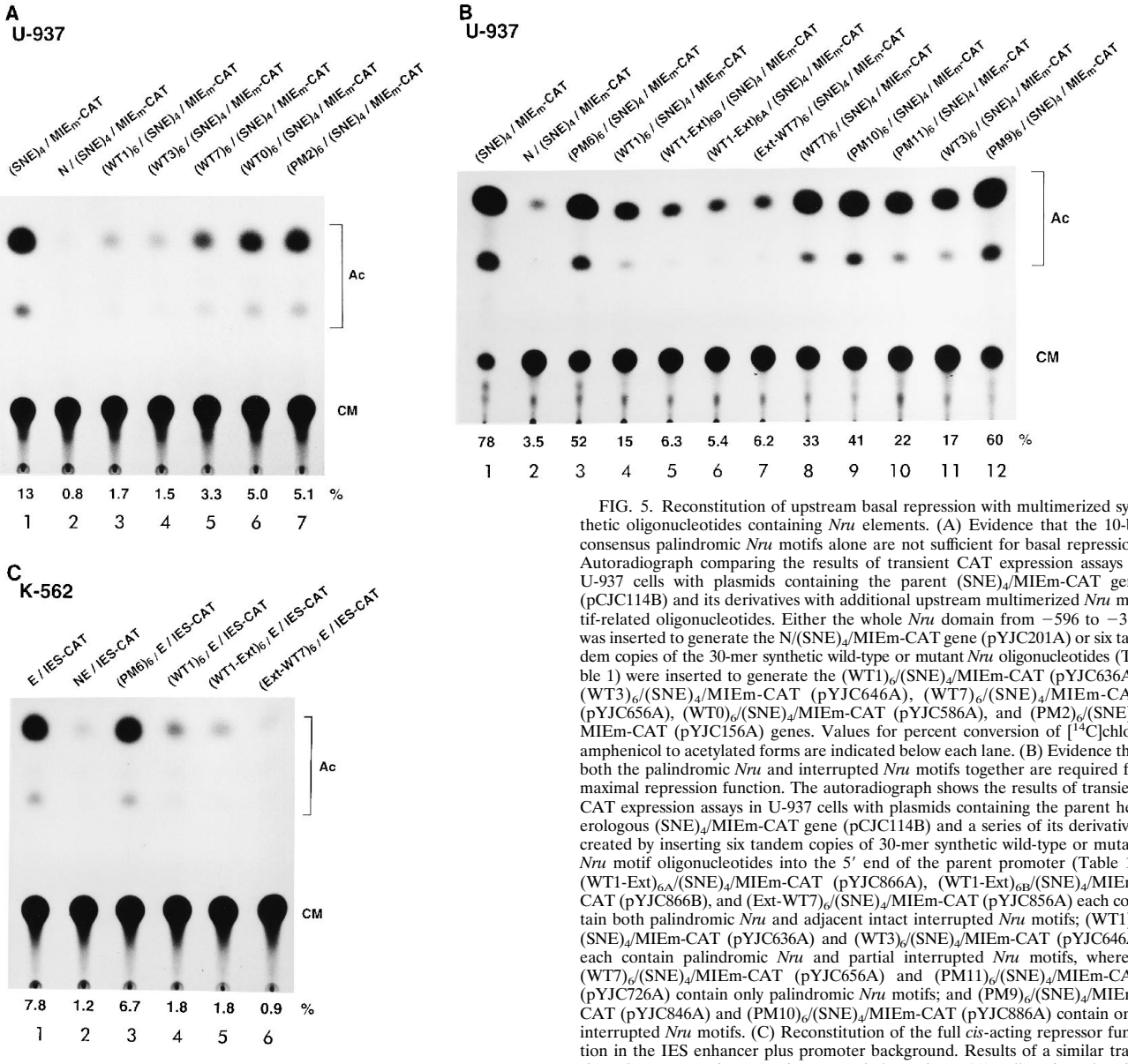

FIG. 5. Reconstitution of upstream basal repression with multimerized synthetic oligonucleotides containing *Nru* elements. (A) Evidence that the 10-bp consensus palindromic *Nru* motifs alone are not sufficient for basal repression. Autoradiograph comparing the results of transient CAT expression assays in U-937 cells with plasmids containing the parent $(SNE)_4$/MIEm-CAT gene (pCJC114B) and its derivatives with additional upstream multimerized *Nru* motif-related oligonucleotides. Either the whole *Nru* domain from −596 to −314 was inserted to generate the N/$(SNE)_4$/MIEm-CAT gene (pYJC201A) or six tandem copies of the 30-mer synthetic wild-type or mutant *Nru* oligonucleotides (Table 1) were inserted to generate the $(WT1)_6$/$(SNE)_4$/MIEm-CAT (pYJC636A), $(WT3)_6$/$(SNE)_4$/MIEm-CAT (pYJC646A), $(WT7)_6$/$(SNE)_4$/MIEm-CAT (pYJC656A), $(WT0)_6$/$(SNE)_4$/MIEm-CAT (pYJC586A), and $(PM2)_6$/$(SNE)_4$/MIEm-CAT (pYJC156A) genes. Values for percent conversion of [^{14}C]chloramphenicol to acetylated forms are indicated below each lane. (B) Evidence that both the palindromic *Nru* and interrupted *Nru* motifs together are required for maximal repression function. The autoradiograph shows the results of transient CAT expression assays in U-937 cells with plasmids containing the parent heterologous $(SNE)_4$/MIEm-CAT gene (pCJC114B) and a series of its derivatives created by inserting six tandem copies of 30-mer synthetic wild-type or mutant *Nru* motif oligonucleotides into the 5′ end of the parent promoter (Table 1). $(WT1\text{-}Ext)_{6A}$/$(SNE)_4$/MIEm-CAT (pYJC866A), $(WT1\text{-}Ext)_{6B}$/$(SNE)_4$/MIEm-CAT (pYJC866B), and $(Ext\text{-}WT7)_6$/$(SNE)_4$/MIEm-CAT (pYJC856A) each contain both palindromic *Nru* and adjacent intact interrupted *Nru* motifs; $(WT1)_6$/$(SNE)_4$/MIEm-CAT (pYJC636A) and $(WT3)_6$/$(SNE)_4$/MIEm-CAT (pYJC646A) each contain palindromic *Nru* and partial interrupted *Nru* motifs, whereas $(WT7)_6$/$(SNE)_4$/MIEm-CAT (pYJC656A) and $(PM11)_6$/$(SNE)_4$/MIEm-CAT (pYJC726A) contain only palindromic *Nru* motifs; and $(PM9)_6$/$(SNE)_4$/MIEm-CAT (pYJC846A) and $(PM10)_6$/$(SNE)_4$/MIEm-CAT (pYJC886A) contain only interrupted *Nru* motifs. (C) Reconstitution of the full *cis*-acting repressor function in the IES enhancer plus promoter background. Results of a similar transient CAT expression experiment carried out in K-562 cells using plasmids containing the parent E/IES-CAT gene (pYJC93A) and a series of inserted upstream oligonucleotides containing 6× multimerized P plus I *Nru* motif derivatives (PM6 in pWPT17A, WT1 in pYJC636A, WT1-Ext in pWPT16A, and Ext-WT7 in pWPT15A) as well as the positive control NE/IES-CAT gene (pYJC94A) that contains the added intact *Nru* domain. Values for percent conversion of [^{14}C]chloramphenicol to acetylated forms are indicated below each lane.

ilarly, the $(Ext\text{-}WT7)_6$/$(SNE)_4$/MIEm-CAT gene contains an intact interrupted *Nru* motif located 5′ to the consensus palindromic *Nru* site 7. The nucleotide sequences of these and five additional inserted mutant *Nru* oligonucleotide motifs (PM6 to PM11) are listed in Table 1.

In transient transfection assays in U-937 cells using these new reagents, both of the enlarged multimerized *Nru* motifs in $(WT1\text{-}Ext)_{6A}$/$(SNE)_4$/MIEm-CAT and $(Ext\text{-}WT7)_6$/$(SNE)_4$/MIEm-CAT gave 12 to 14-fold down-regulation, irrespective of whether the added intact interrupted *Nru* motif lay 3′ or 5′ to the palindromic *Nru* site (Fig. 5B, lanes 6 and 7). Furthermore, either the forward or backward orientation of the enlarged WT1-Ext motif reduced the basal activity equally well (lanes 5 and 6). In the same experiment, the intact *Nru* domain control decreased the basal activity 22-fold compared with that of the parent $(SNE)_4$/MIEm-CAT (Fig. 5B, lanes 1 and 2). Again, both of the target genes containing a palindromic *Nru* motif plus an incomplete interrupted *Nru* motif (WT1 and WT3 inserts) gave only partial repression effects (4.6- to 5.2-fold down-regulation, lanes 4 and 11), whereas that containing the shorter-core 10-bp palindromic *Nru* motif alone (WT7 insert) gave minimal down-regulation (2.3-fold, lane 8). Therefore, the extended palindromic *Nru* motifs with an adjacent, intact interrupted *Nru* motif added either 3′ or 5′ fully restored the ability to down-regulate a high basal heterologous CAT reporter gene in U-937 cells.

The introduction of mutations into the palindromic *Nru* sequence (P) within the WT1 motif nearly totally abolished basal repression in the $(PM6)_6$/$(SNE)_4$/MIEm-CAT gene (Fig. 5B, lane 3). Similarly, the introduction of point mutations into either the palindromic *Nru* motif (P) or the interrupted palindromic motif (I) of the Ext-WT7 oligonucleotide also virtually

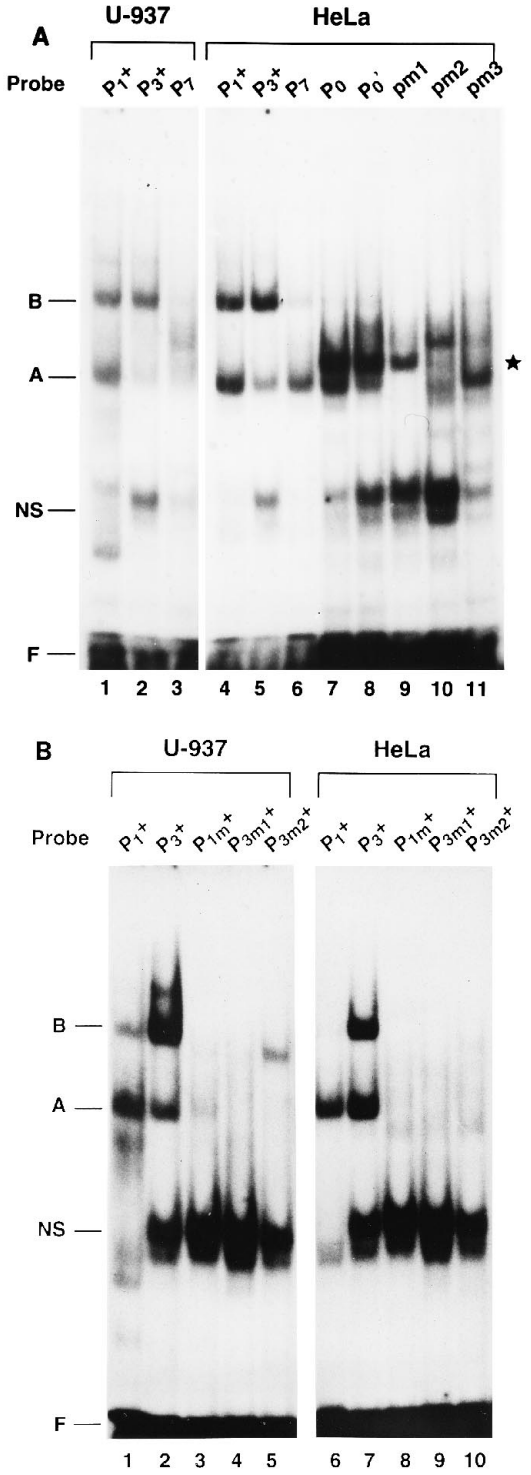

FIG. 6. Identification of two DNA-bound protein complexes that specifically interact with wild-type *Nru* probes. (A) Autoradiograph showing the results of EMSA using a panel of ^{32}P-labelled 30-mer synthetic wild-type or mutant *Nru* oligonucleotide pair DNA probes (Table 1) and nuclear extracts from U-937 cells (lanes 1 to 3) or HeLa cells (lanes 4 to 11). Lanes: 1 and 4, wild-type *Nru* site 1 (LGH1243/1244) probe with palindromic and partial interrupted *Nru* sequences (P_1^+); 2 and 5, wild-type *Nru* site 3 (LGH1245/1246) probe with palindromic and partial interrupted *Nru* sequences (P_3^+); 3 and 6, wild-type *Nru* site 7 (LGH1247/1248) probe with palindromic *Nru* sequences only (P_7); 7 and 8, wild-type *Nru* probes (LGH895/534 and LGH533/534) with a 10-bp consensus palindromic *Nru* motif and randomly selected flanking sequences (P_0 and P_0'); 9, 10, and 11, mutant *Nru* (LGH535/536, LGH647/648, and LGH805/806) probe with mutated palindromic *Nru* sequences (pm1 and pm2) or mutated flanking sequences (pm3). (B) Similar EMSA with another panel of *Nru* oligonucleotide probes. Lanes: 1 and 6, wild-type *Nru* site 1 (LGH1243/1244) probe (P_1^+); 2 and 7, wild-type *Nru* site 3 (LGH1245/1246) probe (P_3^+); 3 and 8, mutant *Nru* site 1 (LGH1249/1250) probe (P_{1m}^+); 4, 5, 9, and 10, two versions of *Nru* site 3 (LGH1251/1252 and LGH1253/1254) with mutations in the core *Nru* palindrome sequence (P_{3m1}^+ and P_{3m2}^+). A and B, specific *Nru* complexes; *, artifactual flanking sequence binding factor; NS, nonspecific binding; F, free probe.

abolished the silencer effect in U-937 cells. In this case, the 12-fold repression by the parent P plus I version in the Ext-WT7 element (lane 7) was reduced to only 2.0- to 3.5-fold repression when either the P or I submotif was mutated (PM10 and PM11 in Fig. 5B, lanes 9 and 10). Interestingly, disruption of the palindromic *Nru* motif within the WT3 element by the insertion of 1 bp to convert it into an interrupted *Nru* motif also abolished the repression function (compare the WT3 insert with PM9 in Fig. 5B, lanes 11 and 12).

We also tested another set of CAT reporter plasmids containing NREs inserted upstream of the NF-κB domain and the IES minimal promoter in the E/IES-CAT background. These were transfected into K-562 cells (Fig. 5C). The results demonstrated that both the PI and IP combinations of the palindromic *Nru* motif plus adjacent interrupted *Nru* motifs also fully restored the down-regulation function of the *Nru* domain in these cells (compare the parent NE/IES-CAT target in lane 2 with the WT1-Ext and Ext-WT7 inserts in lanes 5 and 6). Mutation in the palindromic *Nru* motif again abolished the repression function for $(PM6)_6$/E/IES-CAT (lane 3). Therefore, we conclude that the palindromic *Nru* motifs are absolutely necessary for the silencer activity in the IES minimal plus NF-κB enhancer promoter background but that the flanking interrupted *Nru* motifs are also required to reconstitute the full repression phenotype.

Identification of specific *Nru* motif binding factors in U-937 and HeLa cell nuclear extracts. Since the *Nru* elements exert down-regulation functions, we anticipated that a novel cellular factor might bind to these sites. Therefore, we initially synthesized and end-labelled consensus 30-bp oligonucleotide pair probes representing the core 10-bp palindromic wild-type *Nru* motif with randomly chosen flanking sequences (P_0) or representing a series of point mutants derived from P_0 (pm1, pm2, pm3, pm4, and pm5) (Table 1) and tested them for binding activities in U-937 or HeLa cell nuclear extracts by either direct or competition EMSA. Two versions of the wild-type palindromic *Nru* motif (P_0 and P_0') formed several complexes with HeLa nuclear extracts (Fig. 6A, lanes 7 and 8), and competition with P_0 itself prevented all of these complexes from forming (not shown). Mutations within the 10-bp core *Nru* motif at positions 4, 5, 6, and 7 for pm1 or at positions 2, 3, 8, and 9 for pm2 (Table 1) both abolished formation of one of these complexes (A; Fig. 6A, lanes 9 and 10), but mutation outside of the core *Nru* motif (pm3) failed to do so (lane 11). In contrast, formation of an abundant, but slightly slower migrating complex (labelled with an asterisk) that bound to both P_0 and P_0' was abolished by both the pm2 and pm3 mutations (although not by pm1), implying that it represented an artifactual binding species created by the junction of the core *Nru* motif and the particular flanking sequences used in P_0 (lanes 7, 8, and 9).

Therefore, to avoid this complication, we used new synthetic wild-type oligonucleotide probes containing the core palindromic *Nru* motifs together with their natural context flanking sequences from three of the seven *Nru* sites (P_1^+, P_3^+, and P_7) (Table 1). The results of EMSA experiments using this series of probes showed similar binding patterns in both U-937 and HeLa cell extracts (Fig. 6A, lanes 1 to 6). The wild-type *Nru*

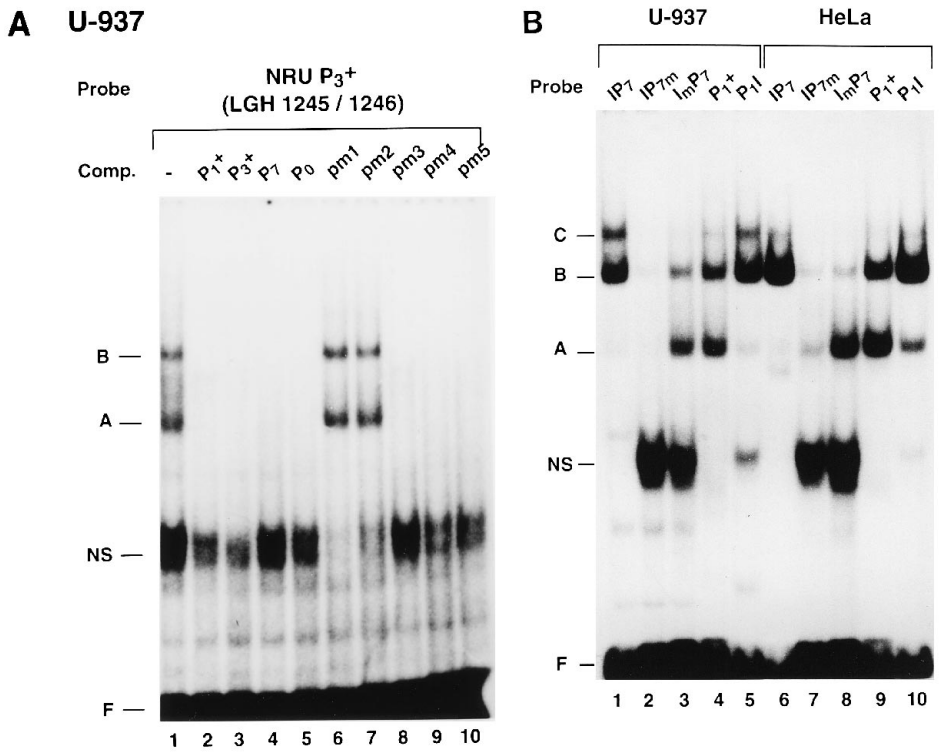

FIG. 7. (A) Evidence that both the A and B complexes bind to the palindromic *Nru* motifs as assayed by competition EMSA. A ^{32}P-labelled annealed wild-type *Nru* site 3 (LGH1245/1246) oligonucleotide probe (P_3^+) was incubated with the U-937 cell nuclear extract in the presence of a 300-fold excess of a series of unlabelled annealed *Nru* motif oligonucleotides (lanes 2 to 10). Lane 1 received an added sample protein without competitor DNA. Lanes: 2, 3, 4, 5, 8, 9, and 10, wild-type 10-bp palindromic *Nru* competitor motifs with different flanking sequences (Table 1); 6 and 7, mutant palindromic *Nru* motif competitors. A and B represent the two *Nru*-specific binding activities; NS, nonspecific binding; F, free probe. (B) Evidence that the interrupted *Nru* motif is required for complex B formation. Autoradiograph showing the results of EMSA using a series of ^{32}P-labelled *Nru* oligonucleotides and nuclear extracts from U-937 cells (lanes 1 to 5) or HeLa cells (lanes 6 to 10). Lanes: 1 and 6, wild-type enlarged site 7 (IP_7; LGH1259/1260) *Nru* probe containing both palindromic and intact interrupted *Nru* sequences; 2 and 7, mutant *Nru* probe (IP_{7m}; LGH1263/1264) modified from IP_7 with a mutated palindromic *Nru* motif; 3 and 8, mutant *Nru* probe (I_mP_7; LGH1265/1266) modified from IP_7 with a mutated interrupted *Nru* motif; 4 and 9, wild-type site 1 (P_1^+; LGH 1243/1244) *Nru* probe containing a *Nru* palindrome and a partial interrupted *Nru* motif; 5 and 10, wild-type enlarged site 1 *Nru* probe (P_1I; LGH1267/1268) modified from P_1^+ containing both palindromic and interrupted *Nru* sequences. A and B, specific *Nru* binding activity; C, higher-order *Nru* binding complex; NS, nonspecific binding; F, free probe.

site 1 (P_1^+) and site 3 (P_3^+) probes each bound (with different relative affinities) to two specific complexes, labelled A and B (lanes 1, 2, 4, and 5), while the wild-type *Nru* site 7 probe (P_7) formed complex A but very little complex B (lanes 3 and 6). To confirm that the palindromic *Nru* motif is required for both the A and B complexes to form, we also tested three more *Nru* probes that were mutated within the core palindromic motifs (P_{1m}^+, P_{3m1}^+, and P_{3m2}^+; Table 1). As expected, both complexes A and B failed to form in samples containing all three mutant oligonucleotide probes (Fig. 6B, lanes 3 to 5 and 8 to 10). In contrast, both of the wild-type *Nru* probes tested (P_1^+ and P_3^+) again formed the A and B complexes (lanes 1, 2, 6, and 7), although P_3^+ proved to bind preferentially to B rather than to A, and P_1^+ formed more of complex A than of B. Therefore, we conclude that both the A and B cellular factors bind specifically to the palindromic *Nru* motifs.

To examine whether one or both of the A and B complexes represent factors that can bind to the palindromic *Nru* motif alone, without influences from the flanking sequences, a competition EMSA experiment was performed with 300-fold excess of each of the initial nine *Nru* oligonucleotide probes. These contained the wild-type 10-bp palindromic *Nru* motif, either with (P_1^+, P_3^+) or without (P_0, P_7) adjacent partial interrupted *Nru* motifs, or variants of P_0 with mutations either inside or outside of the core *Nru* motifs (Table 1). Without any specific unlabelled competitor, the ^{32}P-labelled P_3^+ probe detected bands A and B (Fig. 7A, lane 1) and the addition of an excess of the P_3^+ oligonucleotide itself efficiently competed for binding by both the A and B complexes (Fig. 7A, lane 3). Competition with each oligonucleotide pair containing an intact palindromic *Nru* motif, with or without its natural context flanking sequences (P_1^+, P_7, P_0, pm3, pm4, pm5), also led to a complete loss of both the A and B complexes in all cases (lanes 2, 4, and 5 and 8 to 10). In contrast, the two P_0-derived oligonucleotides containing mutated core palindromic *Nru* motifs (pm1 and pm2) both failed to prevent either complex from forming (lanes 6 and 7). Therefore, these results confirm that the 10-bp palindromic *Nru* motif alone, despite its functional inactivity, can compete fully for the formation of both the A and B complexes (at least on the P_3^+ probe).

The interrupted *Nru* sequence is also required for efficient complex B formation. Although the palindromic *Nru* motifs were clearly required for the formation of all specific DNA-bound complexes, the abundance of the A and B complexes as well as functional down-regulation seemed to be greatly affected by the flanking sequences. To examine the importance of the flanking sequences for complex formation, the four variant *Nru* motif probes containing both P and I motifs (Table 1) were also end labelled and compared with the parent P_1^+ probe in a direct EMSA experiment with both U-937 and HeLa extracts (Fig. 7B). These versions of the NRE included enlarging the flanking sequences of the palindromic *Nru* motif

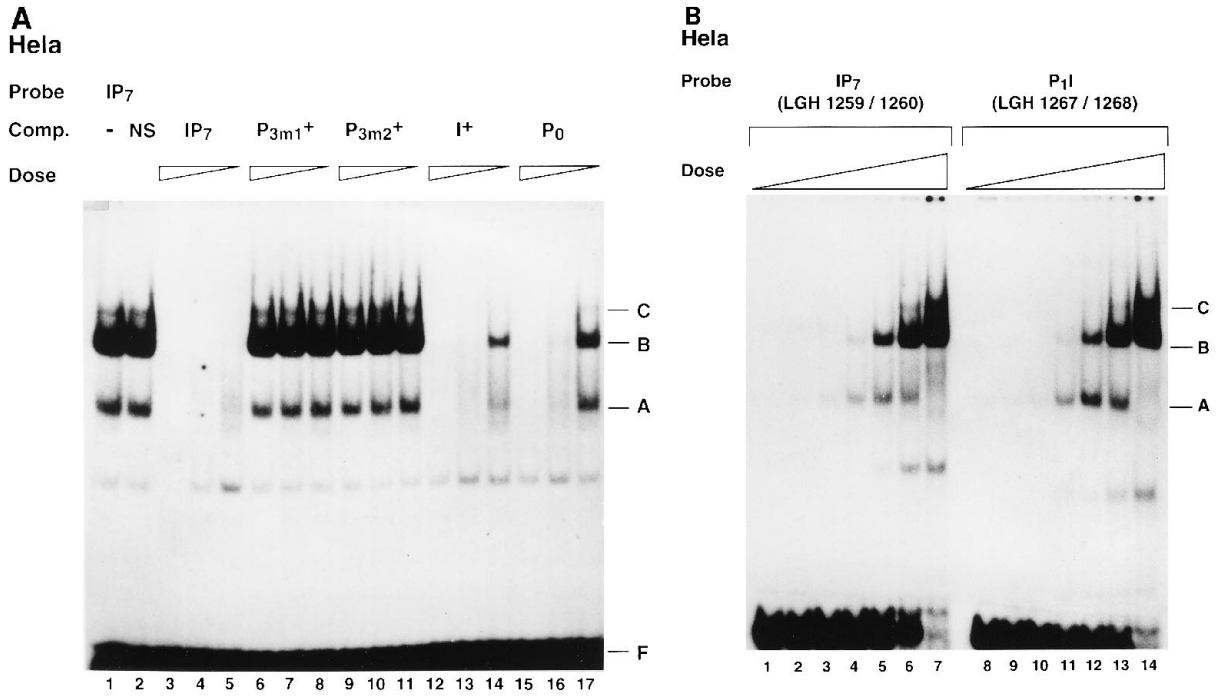

FIG. 8. (A) Evidence that a component of the complex that binds to the palindromic motif also binds to the interrupted motif. Competition EMSA using the ^{32}P-labelled wild-type extended IP_7 *Nru* probe (LGH1259/1260) and HeLa cell nuclear extracts in the presence of excess amounts (300-, 30, and 3-fold) of unlabelled *Nru* motif oligonucleotide competitor DNAs (lanes 3 to 17). Lanes 1 and 2 received added sample protein without any competitor or with a nonspecific competitor (LGH531/532), respectively. Lanes: 3 to 5, wild-type extended site 7 *Nru* motif (IP_7; LGH1259/1260); 6 to 8, mutant site 3 *Nru* motif (P_{3m1}^+; LGH1251/1252); 9 to 11, mutant site 3 *Nru* motif (P_{3m2}^+; LGH1253/1254); 12 to 14, modified site 3 *Nru* motif (I^+; LGH1257/1258) converted into an intact interrupted *Nru* motif; 15 to 17, core consensus palindromic *Nru* sequence only (P_0; LGH 895/534). (B) dose-response relationships between the A, B, and C complexes when bound to the IP and PI probes. Comparison of EMSA results using the two wild-type extended P plus intact I *Nru* probes IP_7 (LGH1259/1260, lanes 1 to 7) or P_1I (LGH1267/1268, lanes 8 to 14) and various amounts of HeLa cell nuclear extract that increased in twofold steps from 0.05 to 3.2 μl.

in P_1^+ and P_7 to encompass the complete adjacent interrupted *Nru* motif sequence TCGNCGA (referred to as I), placed on either the 5′ or 3′ side of the 10-bp palindrome to create the IP_7 or P_1I double motifs. The EMSA results showed that these two NRE probes containing both intact interrupted and palindromic *Nru* motifs resulted in much more complex B formation than occurred with the P_1^+ parent (Fig. 7B, compare lanes 1, 5, 6, and 10 with lanes 4 and 9). Furthermore, the U-937 extract gave rise to the appearance of an even slower mobility complex C with both probes. Mutation within the palindromic *Nru* motif portion of IP_7 abolished formation of both the A and B complexes, despite the fact that an intact I motif was still present (IP_{7m} = PM10; lanes 2 and 7), but mutation in the flanking interrupted *Nru* motif portion of IP_7 dramatically reduced complex B formation (I_mP_7 = PM11; lanes 3 and 8), together with a concomitant increase in the amount of complex A (compare lanes 1 and 3 or lanes 6 and 8). Note that converting the incomplete interrupted *Nru* motif part of the P_1^+ probe into an intact interrupted *Nru* motif to generate the combined P_1I probe produced significantly more complex B (but less complex A) than was bound to the P_1^+ probe (Fig. 7B, compare lanes 4 and 9 with lanes 5 and 10, respectively). Therefore, we conclude that complex A involves recognition of the palindromic *Nru* motif only and that complex B but not A interacts with the interrupted *Nru* palindromic sequence. Indeed, formation of complex B must involve recognition of both the palindromic plus the interrupted *Nru* motif sequences.

To further study the relationship between the band A and B complexes (Fig. 8A), we performed competition EMSA with the HeLa cell nuclear extract by using decreasing doses of unlabelled oligonucleotides representing the extended I plus P *Nru* motif (IP_7), two mutant *Nru* motifs (P_{3m1}^+ and P_{3m2}^+), an intact interrupted *Nru* motif (I^+), and the core palindromic *Nru* motif alone (P_0). Both the P_0 and I^+ oligonucleotide competitors completely prevented formation of both the A and B complexes at 30-fold excess but did so with at least 3- to 10-fold lower efficiency than did the wild-type IP_7 oligonucleotide competitor. In contrast, both of the mutant *Nru* oligonucleotides, P_{3m1}^+ and P_{3m2}^+, failed to inhibit either complex to any extent even at 300-fold excess. These results imply that there must be a common protein component present in both the A and B complexes.

Finally, we performed a dose response EMSA experiment in which the amount of HeLa extract used was increased in twofold steps (Fig. 8B). The A complexes were the first to form at the lower input protein levels on both the IP_7 and P_1I probes followed by both A and B complexes at a higher dose, but complex A was lost concomitantly with formation of both more complex B and also complex C at the highest input protein levels tested. This binding pattern is consistent with the formation of higher-order homo-oligomeric or hetero-oligomeric structures. Evidently, the protein components that form the A and B complexes interact either additively or cooperatively with each other on the extended *Nru* sites, and either multiple units of a single factor or perhaps several distinct but closely related factors with different affinities may be involved.

The *Nru* motif binding factors are cell-type specific. Since CMV infection is highly cell-type specific (28) and cellular factors may play an important role in modifying CMV infectivity, we were interested in knowing whether the *Nru* binding

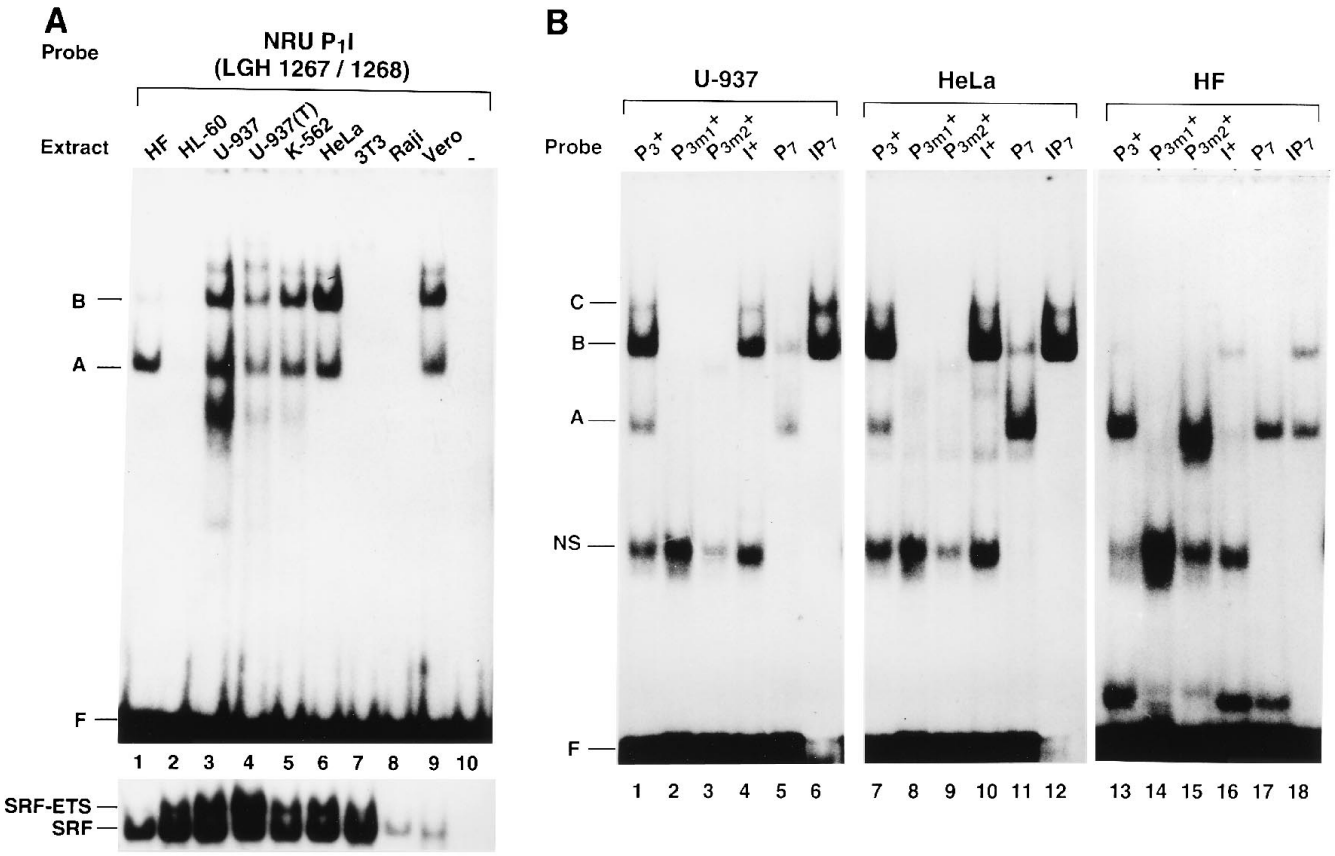

FIG. 9. Differences in cell-type-specific distribution of the *Nru* binding factors. (A) Autoradiograph showing the results of EMSA using a ^{32}P-labelled wild-type extended P plus I *Nru* probe (P_1I; LGH1267/1268) after incubation with 5-μg samples of nuclear extract proteins derived from different cell types. Lanes: 1, HF cells; 2, HL-60 cells; 3, unstimulated U-937 cells; 4, U-937 cells treated with TPA (50 ng/ml) for 18 h; 5, K-562 cells; 6, HeLa cells; 7, BALB/c 3T3 cells; 8, Raji cells; 9, Vero cells. Lane 10 received ^{32}P-labelled probe without any sample protein added. The lower panel shows parallel quality control EMSA bands obtained using a ^{32}P-labelled wild-type HCMV SRF/ETS oligonucleotide probe (SEE; LGH814/815) and the same nuclear extract samples used above. A and B, *Nru*-specific complexes; F, free probe; SRF, DNA-bound SRF or SRF/ETS complexes. (B) Autoradiograph showing the results of EMSA using a panel of five different ^{32}P-labelled 30-mer synthetic wild-type or mutant *Nru* oligonucleotide probes (Table 1) and nuclear extracts from either U-937 (lanes 1 to 6), HeLa (lanes 7 to 12), or HF cells (lanes 13 to 18). Note that the strong new band migrating slightly faster than the A complex on the $P_{3m2}{}^+$ probe in the HF cell extract (lane 15) represents a nonrelevant binding activity associated with this mutated site only and does not correspond to complex A.

factors were present in just a limited subset of cell lineages or in many different cell types. Therefore, EMSA experiments were performed using the parent P_1I wild-type probe with nuclear extracts derived from a variety of different cell types (Fig. 9A). The results showed that both of the specific *Nru* binding complexes A and B can be detected in U-937 cells with or without TPA stimulation, as well as in K-562, HeLa, and Vero cells, when equivalent amounts of nuclear extract (5 μg protein per sample) were used for the assay; however, no such specific complexes were formed in HL-60, BALB/c 3T3, and Raji B-lymphoblast cell extracts, and interestingly, HF cell extracts produced abundant amounts of complex A but very little or no complex B (Fig. 9A, lane 1). Comparison with an internal control consisting of the HCMV MIE overlapping SRF/ETS element probe showed that all of the nuclear extracts retained SRF binding activity (although at reduced levels in the Raji and Vero cell extracts), which argues against the possibility that any of the nuclear preparations that lacked *Nru* binding factors contained either degraded proteins or nonspecific inhibiting factors (Fig. 9A, lower panel).

Additional experiments with several other probes including $P_3{}^+$, P_7, and IP_7 with U-937, HeLa, and HF extracts (Fig. 9B) confirmed that the HF extract appeared to contain a relatively normal amount of the A complex binding factor (lanes 13 and 17), whereas the complex B binding factor was virtually absent even when the IP_7 probe was used (lane 18). Furthermore, the use of the I^+ probe (PM9) here confirmed that conversion of a palindromic *Nru* motif to an interrupted *Nru* motif by a single base pair insertion into $P_3{}^+$ both abolished complex A formation, without affecting the amount of complex B in U-937 and HeLa cell extracts (Fig. 9B, compare lanes 1 and 4 with lanes 7 and 10), and also abolished complex A formation in the HF cell extract (compare lanes 13 and 16). Therefore, complex B does not appear to simply represent two molecules of factor A bound simultaneously.

DISCUSSION

Correlation between *Nru* binding activity and the *cis*-acting down-regulation phenotype. The results of both the in vitro binding assays and our functional assays for basal repression by components of the IES-NRE domain in transfected cells are summarized and correlated in Table 1. Although the multimerized core 10-bp palindromic *Nru* motif alone (P_0) displayed very little silencer function, it was clearly a necessary component for the full repression phenotype because mutations within the core palindromic *Nru* motif itself abolished all negative effects, regardless of the presence of adjacent partial or

complete interrupted *Nru* motifs (compare IP_7, IP_{7m}, and I_mP_7). Nevertheless, the palindromic *Nru* motif alone still formed complex A with both the U-937 and HeLa extracts, and therefore we believe that complex A is necessary, but not sufficient, for the full repression phenotype. On the other hand, the interrupted *Nru* motif alone (I^+) generated complex B only, but again without showing any functional down-regulation effects. The full down-regulatory phenotype required both the palindromic and interrupted *Nru* sequences, which together form complexes A, B, and C with the bipartite probes P_1I and IP_7. Curiously, the intact palindromic *Nru* motif plus an adjacent half-site interrupted *Nru* motif still gave partial repression along with some complex B formation (probes P_1^+ and P_3^+), and P_3^+ was more efficient than P_1^+ at binding to complex B. In summary, the results suggest that additive involvement of binding complexes built up from at least two distinct but probably related protein factor components are required for the full *Nru* domain down-regulation function.

Role of signal transduction pathways in regulation of IES/US3 gene expression. We have also demonstrated here that the bipartite HCMV IES (US3) promoter region (Fig. 10A) contains a proximal basal enhancer (ENH) that can be activated strongly in transient assays by either TPA or OA treatment. Evidently, this portion of the IES control region can detect and respond to changes in the cellular environment without other viral gene products being present. TPA stimulation of the IES ENH domain in U-937 and K-562 cells almost certainly acts through the multicopy NF-κB elements, because responses in our control HIV LTR-CAT target were abolished by mutations of the NF-κB sites and the addition of consensus NF-κB oligonucleotides to heterologous nonresponsive promoters transferred responsiveness in these cell types. We also believe that the OA response is mediated by the NF-κB motifs, because it displays the same pattern as TPA responsiveness with these control targets and because the SCMV MIE region, which lacks any classical NF-κB sites, did not respond. However, the SCMV MIE enhancer is stimulated by TPA induction mediated by both the series III SRF/ETS binding sites (SNE motifs) and by the CRE motifs (4, 9). We initially used OA because of reports that it interfered with the action of phosphatases PP1 and PP2A (10) and altered the function of both the AP-1 transcription factor and MAP kinase (55). More recent reports have suggested that OA induces serine phosphorylation of IκBα and its subsequent proteolytic degradation by a PP2A-dependent mechanism that is different from that mediated by TNFα. However, like TPA and TNFα treatment, this ultimately leads to activation of the Rel/NF-κB heterodimers (51, 58).

The fact that both the IES and MIE enhancer/promoters of HCMV are activated by TPA and OA stimulation via the NF-κB elements leads to the hypothesis that signal transduction pathways triggered by TPA stimulation of protein kinase C or by inhibition of phosphatases such as PP2A may lead to reactivation of the dormant virus from a latent state by simultaneously activating both types of IE genes. We have shown elsewhere that in both HCMV- and SCMV-infected U-937 cells, IE1 mRNA and protein production increases after TPA stimulation and that viral progeny can be found by HF cell cocultivation assays after TPA induction of infected U-937 cells but not uninduced U-937 cells (9). Hence, TPA or other similar signal transduction pathway stimulants may provide the first step in driving the virus into the full lytic replication cascade from a latent state. Studies are in progress to determine whether US3 mRNA and protein levels are also increased under these circumstances.

The US3 gene products associated with the IES enhancer and encoded by its spliced IE transcripts have been reported to be capable of transactivating the cellular hsp70 heat shock gene promoter (11, 54), and heat shock treatment apparently increases both HCMV early antigen and MIE gene transcription (15, 66). Although the US3 gene product is dispensable in permissive infection in tissue culture (21, 23), a deleted HCMV lacking 15 kb of the US region including the IES/US3 gene displays temperature-sensitive characteristics (23) and one of two distinct viral functions that can down-regulate major histocompatibility complex class I expression in HCMV-infected cells has also been mapped to this vicinity (20). Therefore, US3 may potentially be involved either in overcoming stress conditions induced by infection or in evading immune responses, although there is also the more interesting possibility that it plays a key role in vivo in reactivation from a dormant or latent state. Note that herpes simplex virus also contains an IE gene, referred to as IE110 or ICP0, that is dispensible for the lytic cycle in cell culture conditions but appears to be crucial for triggering reactivation both in vivo and in vitro in cell culture models.

Negative *cis*-acting regulatory regions in gene expression. Upstream *cis*-repression motifs are generally thought to be associated with active transcriptional repressor factors, although relatively few (e.g., Krupple, HMG, and yeast α2) have been definitively characterized in either viral or cellular systems (12, 22, 32, 33, 43, 47). In the Epstein-Barr virus (EBV) *Bam*HI-C latency promoter region, there is an upstream EBNA2-responsive element that binds to the cellular CBF1 repressor protein (35). Upon EBV infection, the negative effect of bound CBF1 is converted into positive regulation mediated by protein-protein complex formation with the EBV-encoded EBNA2 transactivator (17). Negative *cis*-acting regulatory regions can potentially maintain genes in a transcriptionally quiescent state, which may be reversed by differentiation or overcome by induction of positive response factors.

Here, we have also identified novel multicopy *cis*-repression motifs, called the *Nru* motifs or *Nru* repressor elements, within the distal segment (NRE) of the HCMV IES promoter control region (Fig. 10A) and have shown that two or more cell-type-specific factors bind to these motifs. Note that the other HCMV enhancer/promoter region (MIE) is associated with two types of *cis*-repression elements: one a presumed active form, perhaps mediated by YY1, within both the far upstream MOD domain and the 21-bp repeats, which contributes to down-regulation in teratocarcinoma stem cells (16, 25, 27, 37, 39), and the other, a likely passive form, in which the IE2 protein produces negative autoregulation by binding to the CRS motif at the start site of the MIE transcription unit (8, 36, 41, 42).

Characterization of the *Nru* binding sites and function of the *Nru* motif. We have narrowed down the minimal elements required for full *Nru* repressor function to be the 10-bp *Nru* palindrome together with an adjacent 7-bp interrupted *Nru* motif. Together, this enlarged bipartite *Nru* repressor element (NRE) allows at least two distinct types of DNA-protein complexes to form possibly in a cooperative fashion. Evidently both types of *Nru* subelements are required for full function and, although they can each bind independently only to either the A (palindromic) or B (interrupted) site binding factors, they each compete for binding to component factors that must be common to both complexes. However, neither the palindromic nor the interrupted *Nru* motifs alone give much down-regulatory activity. Therefore, we hypothesize that some interaction between the two types of protein complexes is required for full function (Fig. 10B) and that the (presumably dimeric) nonre-

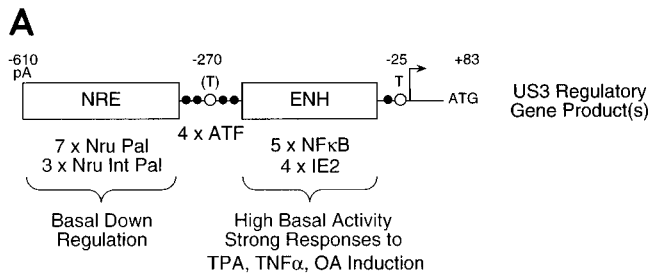

FIG. 10. (A) Summary of the bipartite structural and functional organization of the HCMV IES upstream *cis*-acting control region. Evidence that the proximal enhancer (ENH) domain but not the distal negative *Nru* regulatory domain (NRE) responds to TPA and OA treatment and that the NRE domain, containing multiple *Nru* repressor elements, produces a *cis*-acting basal down-regulation phenotype. As shown here also down-regulation correlates with binding of cellular factors to both the palindromic and interrupted *Nru* motifs within each NRE. Direct evidence that the ENH domain contains five binding sites for cellular NF-κB/Rel class binding factors and four for the HCMV IE2 DNA-binding protein as well as the finding that it responds either positively or negatively to cotransfection with IE2 in different cell types is presented elsewhere (59a). TNFα responsiveness is predicted based on the ability of classical immunoglobulin kappa-like NF-κB motifs to confer this property to heterologous promoters. (B) Diagram illustrating a possible model for *Nru* factor binding to the NRE oligonucleotide sites in the IES negative regulatory domain.

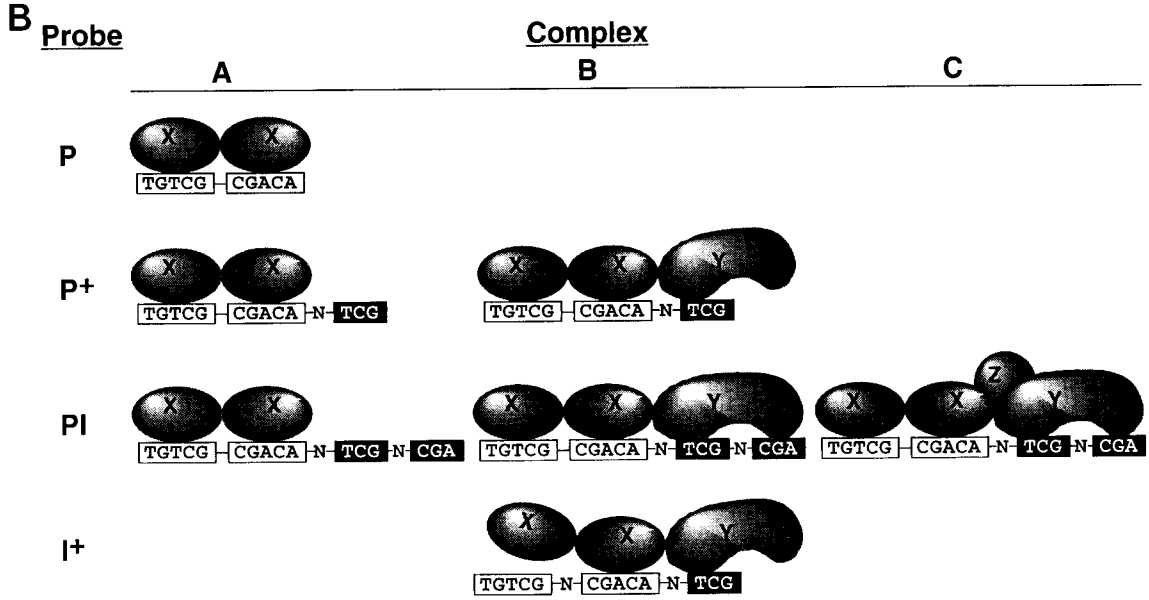

pressing protein subunit (X_2) that recognizes the palindromic *Nru* motif may in turn serve as a base for binding of another protein (Y), which also interacts with the nucleotides of the interrupted *Nru* motif and may contain the active repression domain. Alternatively, the palindromic *Nru* binding protein may itself contain a repressor domain but requires the interrupted *Nru* motif binding factor to help it to bind to the palindromic site with higher affinity or in a correct conformation. Another alternative model suggests that simultaneous binding of these two protein complexes allows access for a third factor (Z) to suppress transcription (complex C), although this may not itself be a direct DNA-binding protein.

Interestingly, if one considers just the pentameric half sites of the palindromic *Nru* motifs as a potential core functional unit here, then the NRE shows considerable resemblance to both the far-upstream MOD domain within the HCMV MIE region and to binding sites for a recently described *Drosophila* BEAF-32 insulator factor (67). The insulator factor binds to boundary sequences between polytene chromosome bands and chromosome puffs that appear to function by blocking the higher-order chromatin reorganization effects of adjacent enhancer or locus control regions (LCRs) on one side of the binding sites from influencing specific gene domains on the other side (59). One defined BEAF-32 binding site bounding the *Drosophila* hsp70 domain contains three copies of the pentamer CGATA within a 34-bp footprinted region (67). Note that most of the CMV half-site *Nru* pentamer motifs are CGACA and that the entire 260-bp *Nru* domain from −561 to −310 contains a cluster of 22 interspersed CGATA or CGA CA motifs, many of which encompass or are adjacent to the palindromic *Nru* sites. Several more potential motifs fit into a relaxed consensus of CGATY, including most of the interrupted sites adjacent to the *Nru* palindromes that also proved to be functionally relevant in our oligonucleotide probe series. Similarly, within the 260-bp MOD region associated with the HCMV MIE enhancer there are 20 copies of either the CGA TA or CGACA pentamer and again some of them are arranged as adjacent pairs or back-to-back interrupted palindromes, although no 10-bp *Nru*-like palindromes are present (62). It now appears that in both cases these may in effect act as insulators to separate or dampen the effects of the chromatin reorganization characteristics of the adjacent strong inducible enhancer domains (which are equivalent to cellular LCRs) from nearby segments of the viral genome. This would likely be of greatest influence during latency or early stages of reactivation from latency, rather than during the lytic cycle.

Cell-specific distribution of the *Nru* site binding factors. Our results show that both the A and B types of *Nru*-specific binding factor complexes can be detected in U-937 cells, either with or without TPA stimulation, as well as in K-562, HeLa, and Vero cells; however, no specific complexes were formed with HL-60, BALB/c 3T3, or Raji cell extracts, and permissive HF cell extracts contained only the A complex palindromic *Nru* binding factor without significant levels of the B complex in-

terrupted palindrome binding factor (Fig. 9). However, the role of this tissue-specific distribution in regulating cellular gene expression is not yet clear, because we have not examined down-regulation in all of these cell types and the cellular *Nru*-binding factor genes have not yet been cloned or sequenced. Nevertheless, since semipermissive U-937 and nonpermissive Vero and HeLa cells all contain both types of *Nru* binding factors, whereas permissive HF cells only contain the A factor, there are hints that the relative amount of B factor compared with A factor may be a critical determinant of IES activity. We have demonstrated elsewhere that the IES enhancer region also contains IE2 binding sites and responds to the IE2 transactivator either positively or negatively depending on the cell type (3, 5). In transient cotransfection assays, IE2 can apparently overcome the *Nru* silencer effect in HF and U-937 cells, but it down-regulates expression from the IES promoter in Vero cells. In addition, we have observed that synthesis of IES mRNA is not detectable in infected nonpermissive BALB/c 3T3 cells under conditions in which the MIE transcripts and both the IE1 and IE2 proteins are expressed efficiently (3, 5). A brief recent report by Biegalke (1) has claimed that the IES promoter can also be down-regulated by IE2 acting through the cap site. Obviously, the complex factors governing whether or not IES-associated transcripts are expressed in parallel with MIE transcripts, rather than being differentially repressed, may be a significant determinant of whether or not lytic cycle progression occurs and is worthy of much further study.

ACKNOWLEDGMENTS

These studies were funded by DHEW grant RO1-AI31454 to G.S.H. from the National Institute of Allergy and Infectious Diseases. Y.-J.C. was a Ph.D. candidate within the Johns Hopkins Pharmacology Training Program NIH 5T32-M07626 and was supported in part by a scholarship from the Ministry of Education, Taiwan, R.O.C.

We thank Sarah Heaggans for assistance in preparation of the manuscript.

REFERENCES

1. **Biegalke, B. J.** 1995. Regulation of human cytomegalovirus US3 gene transcription by a *cis*-repressive sequence. J. Virol. **69:**5362–5367.
2. **Boshart, M., F. Weber, G. Jahn, K. Dorsch-Hasler, B. Fleckenstein, and W. Schaffner.** 1985. A very strong enhancer is located upstream of an immediate early gene of human cytomegalovirus. Cell **41:**521–530.
3. **Chan, Y.-J.** 1996. A model for CMV latency and reactivation: role of cellular factors and signal transduction in transcriptional regulation of the CMV immediate-early gene promoter/enhancer regions. Ph.D. thesis. Johns Hopkins University, Baltimore, Md.
4. **Chan, Y.-J., C. J. Chiou, and G. S. Hayward.** Synergistic interactions between overlapping binding sites for the serum response factor (SRF) and ELK-1 proteins mediate both basal enhancement and phorbol ester responsiveness of primate cytomegalovirus major immediate-early promoters in monocyte and T-lymphocyte cell types. Submitted for publication.
5. **Chan, Y.-J., I. Waheed, and G. S. Hayward.** Unpublished data.
6. **Chang, Y. N., S. Crawford, J. Stall, D. R. Rawlins, K.-T. Jeang, and G. S. Hayward.** 1990. The palindromic series I repeats in the simian cytomegalovirus major immediate-early promoter behave as both strong basal enhancers and cyclic AMP response elements. J. Virol. **64:**264–277.
7. **Chang, Y. N., K.-T. Jeang, C. J. Chiou, Y. J. Chan, M. Pizzorno, and G. S. Hayward.** 1993. Identification of a large bent DNA domain and binding sites for serum response factor adjacent to the NFI repeat cluster and enhancer region in the major IE94 promoter from simian cytomegalovirus. J. Virol. **67:**516–529.
8. **Cherrington, J. M., E. L. Khoury, and E. S. Mocarski.** 1991. Human cytomegalovirus *ie*2 negatively regulates α gene expression via a short target sequence near the transcription start site. J. Virol. **65:**887–896.
9. **Chiou, C. J., Y.-J. Chan, and G. S. Hayward.** Phorbol ester stimulation induces expression from multiple response elements in the major immediate-early enhancer regions of human and simian cytomegalovirus in monocyte and lymphocyte cell types and can lead to activation of the full lytic cycle in non-permissive U-937 cells. Submitted for publication.
10. **Cohen, P., S. Klumpp, and D. L. Schelling.** 1989. An improved procedure for identifying and quantitating protein phosphatases in mammalian tissues. FEBS Lett. **250:**596–600.
11. **Colberg-Poley, A. M., L. D. Santomenna, P. P. Harlow, P. A. Benfield, and D. J. Tenney.** 1992. Human cytomegalovirus US3 and UL36-38 immediate-early proteins regulate gene expression. J. Virol. **66:**95–105.
12. **Cowell, I. G.** 1994. Repression versus activation in the control of gene transcription. Trends Biochem. Sci. **19:**38–42.
13. **de Wet, J. R., K. V. Wood, M. DeLuca, D. R. Helinski, and S. Subramani.** 1987. Firefly luciferase gene: structure and expression in mammalian cells. Mol. Cell Biol. **7:**725–737.
14. **Dignam, J. D., R. M. Lebovitz, and R. G. Roeder.** 1983. Accurate transcription initiation by RNA polymerase II in a soluble extract from isolated mammalian nuclei. Nucleic Acids Res. **11:**1475–1489.
15. **Geelen, J. L., R. Boom, G. P. Klaver, R. P. Minnaar, M. C. Feltkamp, F. J. van Milligen, C. J. Sol, and J. van der Noordaa.** 1987. Transcriptional activation of the major immediate early transcription unit of human cytomegalovirus by heat-shock, arsenite and protein synthesis inhibitors. J. Gen. Virol. **68:**2925–2931.
16. **Gonczol, E., P. W. Andrews, and S. A. Plotkin.** 1984. Cytomegalovirus replicates in differentiated but not in undifferentiated human embryonal carcinoma cells. Science **224:**159–161.
17. **Hsieh, J. J., and S. D. Hayward.** 1995. Masking of the CBF1/RBPJ kappa transcriptional repression domain by Epstein-Barr virus EBNA2. Science **268:**560–563.
18. **Hunninghake, G. W., M. M. Monick, B. Liu, and M. F. Stinski.** 1989. The promoter-regulatory region of the major immediate-early gene of human cytomegalovirus responds to T-lymphocyte stimulation and contains functional cyclic AMP-response elements. J. Virol. **63:**3026–3033.
19. **Jeang, K.-T., M. S. Cho, and G. S. Hayward.** 1984. Abundant constitutive expression of the immediate-early 94K protein from cytomegalovirus (Colburn) in a DNA-transfected mouse cell line. Mol. Cell. Biol. **4:**2214–2223.
20. **Jones, T. R., L. K. Hanson, L. Sun, J. S. Slater, R. M. Stenberg, and A. E. Campbell.** 1995. Multiple independent loci within the human cytomegalovirus unique short region down-regulate expression of major histocompatibility complex class I heavy chains. J. Virol. **69:**4830–4841.
21. **Jones, T. R., and V. P. Muzithras.** 1992. A cluster of dispensable genes within the human cytomegalovirus genome short component: IRS1, US1 through US5, and the US6 family. J. Virol. **66:**2541–2546.
22. **Keleher, C. A., C. Goutte, and A. D. Johnson.** 1988. The yeast cell-type-specific repressor alpha 2 acts cooperatively with a non-cell-type-specific protein. Cell **53:**927–936.
23. **Kollert-Jons, A., E. Bogner, and K. Radsak.** 1991. A 15-kilobase-pair region of the human cytomegalovirus genome which includes US1 through US13 is dispensable for growth in cell culture. J. Virol. **65:**5184–5189.
24. **Kondo, K., H. Kaneshima, and E. S. Mocarski.** 1994. Human cytomegalovirus latent infection of granulocyte-macrophage progenitors. Proc. Natl. Acad. Sci. USA **91:**11879–11883.
25. **Kothari, S., J. Baillie, J. G. Sissons, and J. H. Sinclair.** 1991. The 21bp repeat element of the human cytomegalovirus major immediate early enhancer is a negative regulator of gene expression in undifferentiated cells. Nucleic Acids Res. **19:**1767–1771.
26. **Kouzarides, T., A. T. Bankier, S. C. Satchwell, E. Preddy, and B. G. Barrell.** 1988. An immediate early gene of human cytomegalovirus encodes a potential membrane glycoprotein. Virology **165:**151–164.
27. **LaFemina, R., and G. S. Hayward.** 1986. Constitutive and retinoic acid-inducible expression of cytomegalovirus immediate-early genes in human teratocarcinoma cells. J. Virol. **58:**434–440.
28. **LaFemina, R. L., and G. S. Hayward.** 1988. Differences in cell-type-specific blocks to immediate early gene expression and DNA replication of human, simian and murine cytomegalovirus. J. Gen. Virol. **69:**355–374.
29. **LaFemina, R. L., and G. S. Hayward.** 1983. Replicative forms of human cytomegalovirus DNA with joined termini are found in permissively infected human cells but not in non-permissive Balb/c-3T3 mouse cells. J. Gen. Virol. **64:**373–389.
30. **LaFemina, R. L., M. C. Pizzorno, J. D. Mosca, and G. S. Hayward.** 1989. Expression of the acidic nuclear immediate-early protein (IE1) of human cytomegalovirus in stable cell lines and its preferential association with metaphase chromosomes. Virology **172:**584–600.
31. **Lathey, J. L., and S. A. Spector.** 1991. Unrestricted replication of human cytomegalovirus in hydrocortisone-treated macrophages. J. Virol. **65:**6371–6375.
32. **Lehming, N., D. Thanos, J. M. Brickman, J. Ma, T. Maniatis, and M. Ptashne.** 1994. An HMG-like protein that can switch a transcriptional activator to a repressor. Nature (London) **371:**175–179.
33. **Licht, J. D., M. J. Grossel, J. Figge, and U. M. Hansen.** 1990. Drosophila Kruppel protein is a transcriptional repressor. Nature (London) **346:**76–79.
34. **Lieberman, P. M., J. M. Hardwick, J. Sample, G. S. Hayward, and S. D. Hayward.** 1990. The Zta transactivator involved in induction of lytic cycle gene expression in Epstein-Barr virus-infected lymphocytes binds to both AP-1 and ZRE sites in target promoter and enhancer regions. J. Virol. **64:**1143–1155.
35. **Ling, P. D., D. R. Rawlins, and S. D. Hayward.** 1993. The Epstein-Barr virus immortalizing protein EBNA-2 is targeted to DNA by a cellular enhancer-binding protein. Proc. Natl. Acad. Sci. USA **90:**9237–9241.

36. **Liu, B., T. W. Hermiston, and M. F. Stinski.** 1991. A *cis*-acting element in the major immediate-early (IE) promoter of human cytomegalovirus is required for negative regulation by IE2. J. Virol. **65:**897–903.
37. **Liu, R., J. Baillie, J. G. Sissons, and J. H. Sinclair.** 1994. The transcription factor YY1 binds to negative regulatory elements in the human cytomegalovirus major immediate early enhancer/promoter and mediates repression in non-permissive cells. Nucleic Acids Res. **22:**2453–2459.
38. **Nabel, G., and D. Baltimore.** 1987. An inducible transcription factor activates expression of human immunodeficiency virus in T cells. Nature (London) **326:**711–713.
39. **Nelson, J. A., C. Reynolds-Kohler, and B. A. Smith.** 1987. Negative and positive regulation by a short segment in the 5′-flanking region of the human cytomegalovirus major immediate-early gene. Mol. Cell. Biol. **7:**4125–4129.
40. **O'Hare, P., and G. S. Hayward.** 1984. Expression of recombinant genes containing herpes simplex virus delayed-early and immediate-early regulatory regions and *trans* activation by herpesvirus infection. J. Virol. **52:**522–531.
41. **Pizzorno, M. C., and G. S. Hayward.** 1990. The IE2 gene products of human cytomegalovirus specifically down-regulate expression from the major immediate-early promoter through a target sequence located near the cap site. J. Virol. **64:**6154–6165.
42. **Pizzorno, M. C., P. O'Hare, L. Sha, R. L. LaFemina, and G. S. Hayward.** 1988. *trans*-activation and autoregulation of gene expression by the immediate-early region 2 gene products of human cytomegalovirus. J. Virol. **62:** 1167–1179.
43. **Renkawitz, R.** 1990. Transcriptional repression in eukaryotes. Trends Genet. **6:**192–197.
44. **Rice, G. P., R. D. Schrier, and M. B. A. Oldstone.** 1984. Cytomegalovirus infects human lymphocytes and monocytes: virus expression is restricted to immediate-early gene products. Proc. Natl. Acad. Sci. USA **81:**6134–6138.
45. **Roberts, M. S., A. Boundy, P. O'Hare, M. C. Pizzorno, D. M. Ciufo, and G. S. Hayward.** 1988. Direct correlation between a negative autoregulatory response element at the cap site of the herpes simplex virus type 1 IE175 (α4) promoter and a specific binding site for the IE175 (ICP4) protein. J. Virol. **62:**4307–4320.
46. **Sambucetti, L. C., J. M. Cherrington, G. W. Wilkinson, and E. S. Mocarski.** 1989. NF-kappa B activation of the cytomegalovirus enhancer is mediated by a viral transactivator and by T cell stimulation. EMBO J. **8:**4251–4258.
47. **Smith, M. R., and W. C. Greene.** 1989. The same 50-kDa cellular protein binds to the negative regulatory elements of the interleukin 2 receptor alpha-chain gene and the human immunodeficiency virus type 1 long terminal repeat. Proc. Natl. Acad. Sci. USA **86:**8526–8530.
48. **Stamminger, T., H. Fickenscher, and B. Fleckenstein.** 1990. Cell type-specific induction of the major immediate early enhancer of human cytomegalovirus by cyclic AMP. J. Gen. Virol. **71:**105–113.
49. **Stasiak, P. C., and E. S. Mocarski.** 1992. Transactivation of the cytomegalovirus ICP36 gene promoter requires the α gene product TRS1 in addition to IE1 and IE2. J. Virol. **66:**1050–1058.
50. **Stinski, M. F., and T. J. Roehr.** 1985. Activation of the major immediate-early gene of human cytomegalovirus by *cis*-acting elements in the promoter-regulatory sequence and by virus-specific *trans*-acting components. J. Virol. **55:**431–441.
51. **Sun, S. C., S. B. Maggirwar, and E. Harhaj.** 1995. Activation of NF-kappa B by phosphatase inhibitors involves the phosphorylation of I kappa B alpha at phosphatase 2A-sensitive sites. J. Biol. Chem. **270:**18347–18351.
52. **Taylor-Wiedeman, J., J. G. Sissons, L. K. Borysiewicz, and J. H. Sinclair.** 1991. Monocytes are a major site of persistence of human cytomegalovirus in peripheral blood mononuclear cells. J. Gen. Virol. **72:**2059–2064.
53. **Taylor-Wiedeman, J., P. Sissons, and J. Sinclair.** 1994. Induction of endogenous human cytomegalovirus gene expression after differentiation of monocytes from healthy carriers. J. Virol. **68:**1597–1604.
54. **Tenney, D. J., L. D. Santomenna, K. B. Goudie, and A. M. Colberg-Poley.** 1993. The human cytomegalovirus US3 immediate-early protein lacking the putative transmembrane domain regulates gene expression. Nucleic Acids Res. **21:**2931–2937.
55. **Thevenin, C., S. J. Kim, and J. H. Kehrl.** 1991. Inhibition of protein phosphatases by okadaic acid induces AP1 in human T cells. J. Biol. Chem. **266:**9363–9366.
56. **Thomsen, D. R., R. M. Stenberg, W. F. Goins, and M. F. Stinski.** 1984. Promoter-regulatory region of the major immediate early gene of human cytomegalovirus. Proc. Natl. Acad. Sci. USA **81:**659–663.
57. **Toorkey, C. B., and D. R. Carrigan.** 1989. Immunohistochemical detection of an immediate early antigen of human cytomegalovirus in normal tissues. J. Infect. Dis. **160:**741–751.
58. **Traenckner, E. B., H. L. Pahl, T. Henkel, K. N. Schmidt, S. Wilk, and P. A. Baeuerle.** 1995. Phosphorylation of human I kappa B-alpha on serines 32 and 36 controls I kappa B-alpha proteolysis and NF-kappa B activation in response to diverse stimuli. EMBO J. **14:**2876–2883.
59. **Vazquez, J., G. Farkas, M. Gaszner, A. Udvardy, M. Muller, K. Hagstrom, H. Gyurkovics, L. Sipos, J. Gausz, M. Galloni, et al.** 1993. Genetic and molecular analysis of chromatin domains. Cold Spring Harbor Symp. Quant. Biol. **58:**45–54.

59a. **Waheed, I., Y.-J. Chan, and G. S. Hayward.** Unpublished data.

60. **Weinshenker, B. G., S. Wilton, and G. P. Rice.** 1988. Phorbol ester-induced differentiation permits productive human cytomegalovirus infection in a monocytic cell line. J. Immunol. **140:**1625–1631.
61. **Weston, K.** 1988. An enhancer element in the short unique region of human cytomegalovirus regulates the production of a group of abundant immediate early transcripts. Virology **162:**406–416.
62. **Weston, K., and B. G. Barrell.** 1986. Sequence of the short unique region, short repeats, and part of the long repeats of human cytomegalovirus. J. Mol. Biol. **192:**177–208.
63. **Wu, T. C., W. A. Lee, M. C. Pizzorno, W. C. Au, Y. J. Chan, R. H. Hruban, G. M. Hutchins, and G. S. Hayward.** 1992. Localization of the human cytomegalovirus 2.7-kb major early beta-gene transcripts by RNA in situ hybridization in permissive and nonpermissive infections. Am. J. Pathol. **141:**1247–1254.
64. **Wu, T. C., M. C. Pizzorno, G. S. Hayward, S. Willoughby, D. A. Neumann, N. R. Rose, A. A. Ansari, W. E. Beschorner, K. L. Baughman, and A. Herskowitz.** 1992. In situ detection of human cytomegalovirus immediate-early gene transcripts within cardiac myocytes of patients with HIV-associated cardiomyopathy. AIDS **6:**777–785.
65. **Yamanishi, K., and F. Rapp.** 1979. Induction of host DNA synthesis and DNA polymerase by DNA-negative temperature-sensitive mutants of human cytomegalovirus. Virology **94:**237–241.
66. **Zerbini, M., M. Musiani, and M. La Placa.** 1985. Effect of heat shock on Epstein-Barr virus and cytomegalovirus expression. J. Gen. Virol. **66:**633–636.
67. **Zhao, K., C. M. Hart, and U. K. Laemmli.** 1995. Visualization of chromosomal domains with boundary element-associated factor BEAF-32. Cell **81:** 879–889.